Master's thesis

NTNU
Norwegian University of Science and Technology
Faculty of Engineering
Department of Energy and Process Engineering

Iselin Ørbek Eide

# Particulate Matter and Dust Deposition in Norwegian Schools:

## Patterns and Implications

Master's thesis in Energy and Environmental Engineering
Supervisor: Dr. Guangyu Cao
Co-supervisor: Azimil Gani Alam (NTNU), Christer Eskedal (N3), Kent Hart (NAAF) and Kai Gustavsen (NAAF)
June 2024

NTNU
Norwegian University of Science and Technology

Iselin Ørbek Eide

# Particulate Matter and Dust Deposition in Norwegian Schools:

## Patterns and Implications

Master's thesis in Energy and Environmental Engineering
Supervisor: Dr. Guangyu Cao
Co-supervisor: Azimil Gani Alam (NTNU), Christer Eskedal (N3), Kent Hart (NAAF) and Kai Gustavsen (NAAF)
June 2024

Norwegian University of Science and Technology
Faculty of Engineering
Department of Energy and Process Engineering

NTNU
Norwegian University of
Science and Technology

# Preface

This thesis was conducted during the spring semester of 2024 and concludes my Master's degree in Energy and Environmental Engineering at the Norwegian University of Science and Technology (NTNU).

The research results from cooperation with N3 and The Norwegian Allergy and Asthma Association. The primary data relied on N3's expertise in collection and data handling. I am grateful to Christer Eskedal, the representative from N3, for generously dedicating time and resources to offer invaluable guidance and share pertinent data. I also extend my appreciation to the representatives from The Norwegian Allergy and Asthma Association, Kent Hart and Kai Gustavsen, for their valuable information and guidance.

I commend Azimil Gani Alam for his guidance and help throughout the thesis, and I also wish to express my gratitude to my project supervisor, Dr. Guangyu Cao, for his consistent guidance and inspiration throughout this process.

Lastly, I would like to thank my cat, Bottas, for keeping me company while I wrote this thesis. He has been a loyal companion, always sleeping on my desk in front of the monitor.

# Abstract

Cleaning routines are traditionally scheduled based on the type of building, how many people use it, and the activities taking place there. However, this type of scheduled cleaning has several limitations. Some areas may be cleaned too often, which wastes resources, while others may not be cleaned sufficiently, which can degrade indoor air quality. This underscores the necessity for a more adaptable and responsive cleaning strategy that adjusts to the actual conditions inside the building.

The study aims to quantify and characterize the correlation between airborne particles and particle deposition in Norwegian schools, with the ultimate goal of modernizing the cleaning industry. By establishing a link between particulate matter levels and particle deposition, cleaning can transition from scheduled routines to an as-needed basis, thereby enhancing productivity and reducing costs.

Measurements obtained using the BM dust detector revealed varying results, with dust coverage occasionally being lower on Friday than on Wednesday despite no cleaning occurring in between. This anomaly is unlikely to be due to high resuspension rates, as no factors were recorded that could cause increased resuspension. The elevated measurements on Wednesday were likely due to measurement error, with a longer four-day interval deemed more accurate, rather than the two-day interval. The IAQ sensor data indicated that a significant portion of the overall particulate matter (PM) was smaller in size, with PM2.5 percentages in the high eighties, except in one room where larger particles predominated. This discrepancy suggests potential measurement errors from the IAQ sensor.

Particle sizes were used to calculate particle deposition rates, which aligned with expected values from previous studies. This demonstrates the feasibility of using IAQ sensors to estimate particle deposition rates. With more detailed readings on particle sizes, it is possible to calculate real-time dust deposition using recorded PM values in the room.

The calculated deposition rates involve more assumptions compared to those derived from literature. For more precise calculations, tests on the elemental composition of particulate matter are necessary to determine the exact weight needed for flow rate calculations. However, this process is costly and time-consuming, undermining the efficiency of using IAQ sensors for dust coverage estimation.

In conclusion, IAQ sensors can provide valuable insights into particle deposition rates, but improving the accuracy of particle size calculations and mass measurements is crucial. Enhanced testing of elemental composition and obtaining more detailed sensor readings will refine these calculations, enabling real-time dust deposition monitoring. This advancement could significantly optimize cleaning schedules, increase productivity, and reduce costs in Norwegian schools.

# Sammendrag

Rengjøringsrutiner er tradisjonelt basert på bygningstype, hvor mange som bruker bygningen, og hvilke aktiviteter som foregår i den. Rengjøringsrutiner som er utarbeidet på bakgrunn av dette har flere begrensninger. Noen områder kan bli rengjort for ofte, noe som sløser med ressurser, mens andre kanskje ikke blir tilstrekkelig rengjort, noe som kan forårsake dårlig inneklima. Dette understreker nødvendigheten av en mer tilpasningsdyktig og responsiv rengjøringsstrategi som justerer seg etter det faktiske behovet i bygningen.

Studien har som mål å kvantifisere og karakterisere sammenhengen mellom luftbårne partikler og partikkelavsetning i norske skoler, med modernisering av rengjørigsbransjen som det endelige målet. Ved å etablere en kobling mellom nivåene av partikler i luften og partikkelavsetning, kan rengjøring gå fra å bli utført på bestemte tidspunkt til behovsbasert rengjøring, noe som øker produktiviteten og reduserer kostnadene.

Målinger utført med BM dustdetector viste varierende resultater, med til tider lavere støvdekning på fredag sammenlignet med onsdag, til tross for mangel på rengjøring i mellomtiden. Denne anomalien skyldes sannsynligvis ikke gjensuspensjon, da det ikke ble registerert aktivitet som kunne foråsaket økt oppvirvling. De forhøyede målingene på onsdag skyldes sannsynligvis målefeil, et lengre firedagers intervall ble vurdert som mer nøyaktig enn todagers intervallet. Data fra IAQ-sensoren indikerte at en betydelig del av den totale partikkelmengden (PM) var av mindre størrelse, med PM2.5-prosentandeler opp mot 80 prosent, bortsett fra i ett rom hvor større partikler dominerte. Dette avviket antyder potensielle målefeil fra IAQ-sensoren.

Partikkelstørrelsene fra IAQ-sensorene ble brukt til å beregne partikkelavsetningshastigheter, som samsvarte med forventede verdier fra tidligere studier. Dette viser at det er mulig å bruke IAQ-sensorer for å estimere partikkelavsetningshastigheter. Med mer detaljerte målinger av partikkelstørrelser, kan det være mulig å beregne støvavsetning i sanntid ved hjelp av registrerte PM-verdier i rommet.

De beregnede avsetningshastighetene involverer flere antakelser sammenlignet med avsetningshastighetene som er hentet fra litteraturen. For mer presise beregninger er det nødvendig med tester av den elementære sammensetningen av partiklene for å bestemme den eksakte massen som trengs for å beregne flytverdien for avsetningen. Denne prosessen er imidlertid kostbar og tidkrevende, noe som undergraver effektiviteten ved å bruke IAQ-sensorer for å finne støvdekning.

IAQ-sensorer gir gode estimater på partikkelavsetningshastigheter, men det er avgjørende å forbedre nøyaktigheten av beregningene om partikkelstørrelse og massemålinger. Forbedret testing av elementær sammensetning og innhenting av mer detaljerte sensoravlesninger vil forbedre disse beregningene, slik at sanntidsovervåking av støvavsetning blir mulig. Denne utviklingen kan betydelig optimalisere rengjøringsrutiner, øke produktiviteten og redusere kostnadene i norske skoler.

# Contents

# List of Figures



# List of Tables

# List of Abbreviations

**HEPA filter** high-efficiency particulate air filter

**HVAC** Heating, Ventilation, and Air Conditioning

**IAQ** Indoor Air Quaity

**IoT** Internet of Things

**LED** Light-Emitting Diode

**NTNU** Norwegian University of Science and Technology

**PM** Particulate Matter

**ppm** Parts Per Million

**RH** Relative Humidity

# List of Symbols

## Latin Symbols

$C_c$ Slip correction factor

$C_{ext}$ Outdoor concentration of particles [µ$g/m^3$]

$C_{Di}$ Concentration of resuspended particles [µ$g/m^3$]

$C_i$ Indoor concentration of particles [µ$g/m^3$]

$D_c$ Dust coverage [%]

$D_e$ Deposition [$kg/(m^3 \cdot s)$]

**f** Infiltration coefficient [1/h]

**Fd** Drag force [N]

**Fe** External body force [N]

**Fg** Gravitational force [N]

**g** Gravitational acceleration [m/s$^2$]

**J** Flow density [$kg/(m^3 \cdot s)$]

**t** time [s]

**r** Radius of particle [m]

**S** Surface area [$m^2$]

$S_i$ Strength of particle sources [µ$g/m^3h$]

$u_f$ Gas velocity [$m/s$]

$u_p$ Particle velocity [$m/s$]

**V** Volume [$m^3$]

**v** Velocity of particle [m/s]

$\mathbf{v}_t$ Termal velocity [m/s]

$V_d$ Speed of deposition [$m/s$]

**X** Dynamic shape factor

## Greek Symbols

$\lambda$ mean free path of air

$\lambda_d$ Combined rate of deposition and resuspension [$1/h$]

$\lambda_{de}$ Rate of deposition [$1/h$]

$\lambda_p$ Rate of penetration [$1/h$]

$\lambda_R$ Rate of resuspension [$1/h$]

$\eta$ Dynamic viscosity [Ns/m$^2$]

$\phi$ Dust load [µ$g/m^3h$]

# List of Definitions

**Adhesion Force** Adhesion force is the attraction that causes different substances to stick together upon contact, operating at the molecular or atomic level.

**Aerosol** An aerosol is a suspension of fine particles or droplets in a gas or liquid medium, often including airborne substances like dust or pollutants.

**Alveoli** Alveoli are small air sacs in the lungs where oxygen and carbon dioxide exchange occurs, crucial for efficient respiratory function.

**Bioaerosol** A bioaerosol is a suspension of airborne particles that contain or are derived from living organisms.

**Boundary layer**A boundary layer is a thin layer of fluid in immediate contact with a solid surface where effects of viscosity are significant, leading to a gradient in velocity between the moving fluid and the stationary surface.

**Capillary Forces** Capillary forces are the interactions between a liquid and a solid surface in narrow spaces or capillaries. Capillary Forces is a combination of adhesive and cohesive forces.

**Cardiovascular** The cardiovascular system, also known as the circulatory system, consists of the heart and blood vessels.

**Cilia** Cilia are tiny hair-like structures on cell surfaces, particularly in the respiratory and reproductive systems, that move in coordinated waves to transport substances.

**Free stream** free stream refers to a region of fluid outside of the boundary layer, where the effects of viscosity are negligible and the flow velocity is essentially undisturbed by the presence of solid objects.

**Hydrodynamic forces** Hydrodynamic forces are the forces exerted by fluids (liquids and gases) in motion on objects within them or on their boundaries.

**Meniscus** A meniscus refers to the curved surface of a liquid, typically water, in a container. It forms a concave or convex shape at the liquid-air interface due to surface tension and adhesive or cohesive forces.

**Mucus** Mucus is a slimy secretion produced by mucous membranes in various body parts, like the respiratory and digestive systems. It traps and eliminates particles, moisturizes, and protects organ linings.

**Quasi-static model** A quasi-static model refers to an analytical approach in which a system is assumed to change so slowly that at any given instant, it can be considered to be in equilibrium.

**Thermophoretic forces** Thermophoretic forces are the forces that cause particles in a fluid to move in response to a temperature gradient. This phenomenon typically results in particles moving from regions of higher temperature to regions of lower temperature.

**Waals attractive forces** Waals attractive forces, or Van der Waals forces, are weak intermolecular forces that include London dispersion forces, dipole-dipole interactions, and dipole-induced dipole forces. These forces arise from temporary or permanent dipoles in molecules, leading to attraction between them.

# 1 Introduction

The introduction begins with a background on current practices and their limitations, followed by a detailed research question, divided into practical implications, assumptions, and limitations. The structure and outline of the work are then briefly described and visualized.

## 1.1 Background and Previous Research

Currently, cleaning routines follow a set schedule based on factors like building type, occupancy, or activities within the premises. This traditional method of cleaning has some clear drawbacks. Rooms might get cleaned unnecessarily, wasting resources, or they might not be cleaned enough, potentially harming indoor air quality. These issues highlight the need for a more flexible and responsive approach to cleaning, one that adapts to real-time conditions within indoor environments.

To address these problems, there's a growing push to explore innovative solutions using sensor technology and data-driven decision-making. By incorporating real-time data on airborne particle levels, cleaning routines can be adjusted strategically, focusing efforts exactly where and when they're needed most. This shift can make cleaning practices more effective and significantly improve the well-being of people indoors.

It's important to consider the broader context of these innovations. People spend a significant portion of their lives indoors—up to 90% according to some studies—making the quality of indoor environments crucial to overall health and well-being [1]. Improving indoor environmental quality globally is a major concern, involving factors like air quality, lighting, acoustics, and thermal comfort. In this context, indoor air quality (IAQ) in schools is particularly important. Schools are where young people spend a lot of their time, and ensuring these spaces are clean and safe directly impacts their health, cognitive function, and academic performance [2].

The urgency of tackling indoor air quality issues is heightened by growing concerns over outdoor air pollution. Outdoor air quality significantly affects indoor environments, especially in urban areas where pollutants can easily enter buildings [3]. This connection underscores the need for a comprehensive approach to air quality management, considering both external and internal factors that affect the air quality experienced by occupants.

As the world continues to face these complex challenges, integrating smart technologies and data-driven strategies into cleaning and maintenance routines offers a forward-thinking solution. By aligning cleaning practices with real-time environmental conditions and prioritizing areas of greatest need, resources can be used more efficiently, indoor air quality can be improved, and the health and well-being of all indoor occupants can be enhanced.

This study builds on previous research that identified a strong correlation between outdoor and indoor particulate matter (PM) levels, highlighting the significant impact of outdoor sources on indoor air quality [4]. Various outdoor influences, from local weather to distant events like sandstorms, were examined. The study analyzed PM10 levels in different locations and classrooms in Norway, considering factors such as seasonal effects, ventilation, and cleaning methods.

A random forest regression algorithm was used to predict indoor PM10 concentrations, considering parameters like relative humidity, temperature, and $CO_2$. The models achieved high accuracy, with $R^2$ values up to 0.92. Key factors influencing indoor PM10 levels included outdoor temperature, outdoor PM levels, and indoor relative humidity, with indoor $CO_2$ consistently significant.

The accurate prediction of indoor PM10 levels suggests potential for forecasting dust deposition and improving cleaning procedures. This study aims to further explore the relationship between PM concentrations and dust deposition indoors.

## 1.2 Research Question and Framework

This section outlines the core research question and the framework within which the study was conducted. The section also details the practical implications, methodological simplifications, and limitations of the study, providing a clear context for the research findings.

### 1.2.1 Research Question

The study aims to quantify and characterize the correlation between airborne particles and particle deposition in Norwegian schools, with the goal of predicting deposition rates from sensor data and ultimately modernizing the cleaning industry. The main research question focuses on understanding how airborne particulate matter levels relate to the deposition of these particles on surfaces.

By identifying and analyzing this correlation, it becomes possible to implement a more efficient cleaning strategy by predicting dust levels based on airborne particulate matter levels. Instead of adhering to rigid cleaning schedules, facilities can adopt an as-needed cleaning approach based on real-time data. This shift has the potential to significantly enhance productivity by directing cleaning efforts where and when they are most necessary, thus ensuring the optimal use of resources. Additionally, this method can lead to substantial cost savings by reducing unnecessary cleaning activities and allowing for better allocation of labor and materials.

### 1.2.2 Practical Implications

The research's practical implications could significantly impact cleaning procedures within indoor environments. By understanding how airborne particulate matter values influence deposition rates, those responsible for maintaining indoor spaces, both organizations and individuals, can refine their practices to achieve better results.

An understanding of the interplay between ventilation systems, particle deposition, and cleaning practices offers a comprehensive approach to enhancing indoor air quality. The utilization of sensor data facilitates data-driven decision-making in cleaning procedures. Rather than adhering to predetermined schedules, cleaning activities can be customized based on real-time information regarding airborne particle levels and other parameters. This ensures that cleaning efforts are concentrated where and when they are most essential, leading to a more efficient allocation of resources.

### 1.2.3 Simplifications and Assumptions

In the study, certain simplifications and assumptions were made to manage complexities and facilitate data analysis. One of the simplifications involved the equations used in the analysis. To make the mathematical modeling more manageable, some of the more complex variables were simplified, which may impact the precision of the results. A significant assumption was that the rate of deposition of particulate matter remained constant between measurements. This assumption was necessary due to the logistical constraints of continuous monitoring but overlooks potential fluctuations in deposition rates caused by varying environmental conditions or indoor activities.

Assumptions about particle sizes were also made. Although some data on particle size was available, the average size of particulate matter had to be estimated based on the total data for PM10 and PM2.5. This approach assumes a uniform distribution within these size ranges, potentially oversimplifying the actual size distribution of the particulate matter in the environment.

The study also assumed weights of particulate matter based on literature values. This assumption relies on the applicability of these literature values to the specific conditions of the study site, which may not always hold true.

### 1.2.4 Limitations and Delimitations

In examining the limitations and delimitations of this study, several factors that could influence the outcomes and interpretations must be acknowledged. The study was constrained by a small sample size, with testing spanning only three weeks and involving a limited number of foil samples. This brief duration and small scope may not fully capture the variability or establish generalizable results.

Time constraints also played a significant role, as the entire assignment was confined to a 20-week period. This limitation likely impacted the depth and extent of the investigations that could be carried out within this timeframe. Furthermore, resource limitations were a critical factor; the absence of necessary equipment to test the elemental composition of particulate matter meant that certain chemical analyses could not be performed, potentially omitting important data regarding the sources or health implications of the PM. This could also impact the calculations done regarding deposition rates.

Since the study was conducted in a single school, the specific environmental conditions, building characteristics, and student behaviors observed may not represent those of other schools or different educational settings. Each of these limitations must be considered when interpreting the findings and could serve as areas for improvement or focus in future studies.

## 1.3 Outline of Thesis

The structure of this thesis is designed to provide a clear and orderly presentation of the research, the outline is illustrated in Figure 1.1. The first section, the introduction, lays the foundation with a description of the background, research question, and scope. The literature review further supports the thesis by providing a comprehensive basis for the research. This section delves into the relevant theory, highlighting crucial aspects such as health risks associated with particulate matter, regulations and guidelines to prevent dangerously high levels of particulate matter, and the dynamics and sources of particulate matter. The theoretical basis explains the key mathematical models and equations used in the thesis. The methodology chapter details the measurement techniques and theoretical calculations. The results chapter encompasses all the findings of the study, which are then discussed in the discussion chapter. Finally, the conclusion addresses the research question and summarizes the findings.

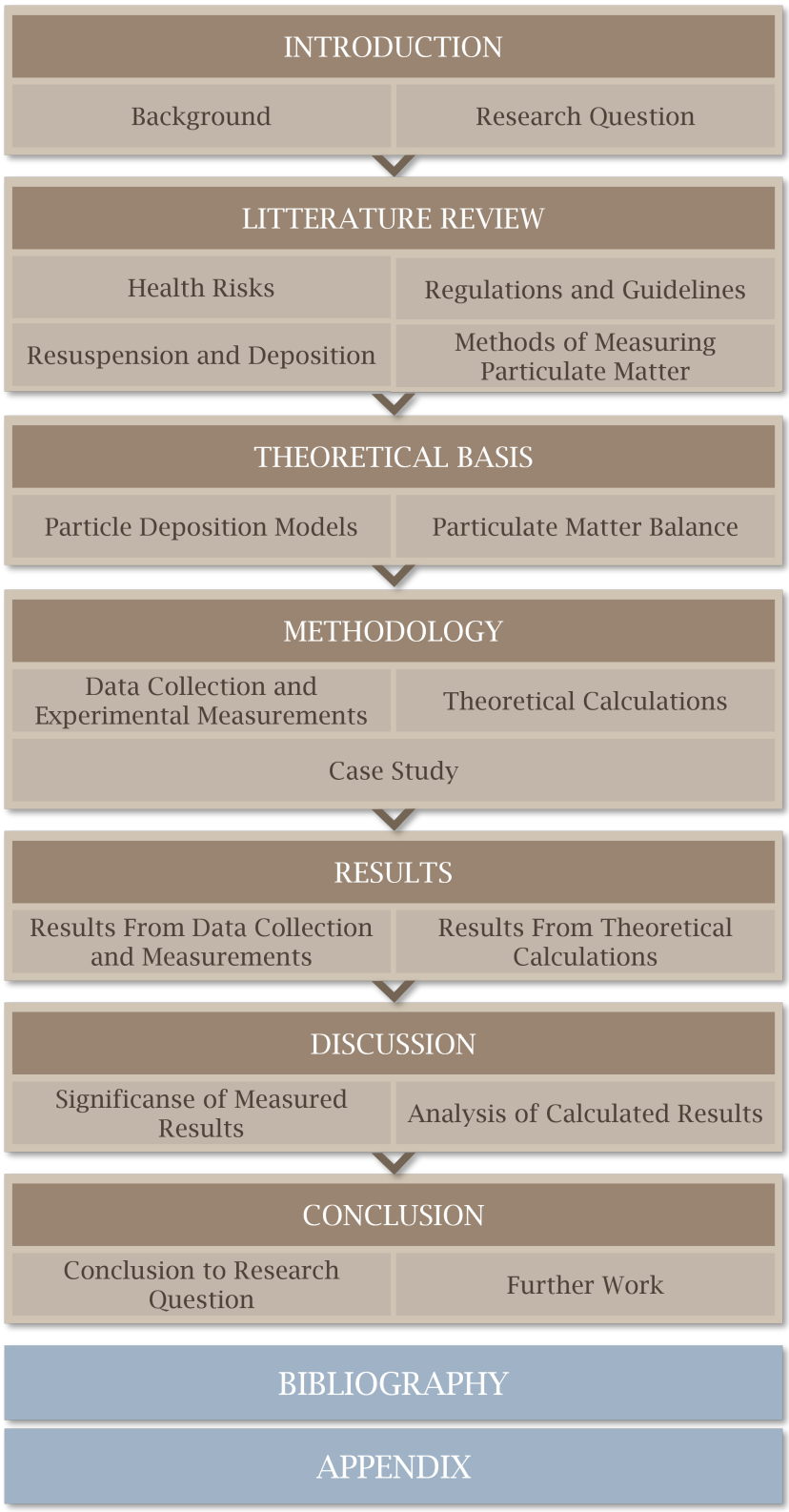


Figure 1.1: Outline of thesis

# 2 Literature Review

The literature review starts by exploring the health risks associated with exposure to particulate matter and then examines how it settles and what influences this, such as external factors and air dynamics. Additionally, existing advice and regulations for managing PM levels are reviewed. Various methods for measuring particulate deposition and concentrations are presented, highlighting techniques like the gravimetric method and light scattering. The goal is to provide a solid understanding of the challenges posed by PM, its impact on health, and strategies for mitigation.

## 2.1 Health Risks Related to Particulate Matter

In 2020, a literature survey highlighted strong positive associations between exposure to fine and ultrafine particles and various health risks, including cardiovascular issues, hypertension, obesity, type 2 diabetes mellitus, cancer, and mortality [2].

While the impact of particulate matter exposure depends on individual physical characteristics such as breathing mode, rate, and volume, the size of particles is directly implicated as the primary cause of health problems [5][6]. Generally, smaller particles tend to penetrate the respiratory tract more deeply. During nasal breathing, cilia and mucus effectively filter particulates larger than 10 µm in diameter (coarse PM). Coarse PM tends to lodge in the trachea or bronchi due to their settling characteristics [7].

Upon inhalation, coarse PM is initially collected in the nose and throat, triggering bodily reactions like sneezing and coughing to eliminate these particles. However, particles less than 10 µm in diameter have the most significant impact on human health. These particles can penetrate the respiratory tract, from nasal passages to alveoli deep within the lungs, affecting gas exchange and potentially even breaching the lung barrier. Eventually, these fine particles can enter the bloodstream, leading to severe health problems [8].

## 2.2 Recommendations, Regulations and Guidelines

As of yet, there are no laws regarding particulate matter in Norwegian buildings; however, there are several recommendations, regulations, and guidelines that are followed when constructing or renovating buildings or during their maintenance.

### 2.2.1 Suggestions and Regulations for Particulate Matter

While there are no official regulations regarding indoor PM values, several suggestions and regulations concerning the indoor and outdoor environment exist. The Building Acts and Regulations (TEK17) state that indoor air quality is influenced by the quality of the outdoor air. Consequently, the regulation requires that the quality of outdoor air be considered in the placement and design of the building, the air intake, and the ventilation system.

Based on the national limits for particulate matter, areas are divided into green, yellow, and red zones. The green zone is defined as having values stricter than those indicated for the yellow zone [9]. The zoning criteria can be viewed in Table 2.1.

Table 2.1: Criteria for zoning in the planning of construction - TEK17 § 13-1

| **Pollution** | **Yellow zone** | **Red zone** |
|---|---|---|
| PM10 | 35–50 µg/m$^3$, 7 days per year | > 50 µg/m$^3$, 7 days per year |

Additionally, the Regulation on the Limitation of Pollution (Forurensningsforskriften) § 7-9 on limit values states that the concentration of pollution in outdoor air shall not exceed the limit values in Table 2.2 more than the permitted number of times [10].

Table 2.2: The concentration of pollution in outdoor air, limit values - Forurensningsforskriften §7-9.

| | **Daily average µg/m$^3$** | **Annual average µg/m$^3$** | **Times above limit** |
|---|---|---|---|
| **PM10** | 50 | 20 | 35 |
| **PM2.5** | | 10 | |

In 2023, the Norwegian Institute of Public Health (Folkehelseinstituttet) and the Norwegian Environment Agency (Miljødirektoratet) revised the air quality criteria for exposure to particulate matter (PM2.5 and PM10), establishing the air quality criteria seen in Table 2.3 [11].

Table 2.3: Air quality criteria set by the Norwegian Institute of Public Health and the Norwegian Environment Agency.

| | **Daily average µg/m$^3$** | **Annual average µg/m$^3$** |
|---|---|---|
| **PM10** | 30 | 15 |
| **PM2.5** | 15 | 5 |

### 2.2.2 Regulations for Cleanliness

NS-INSTA 800 is a system for determining and assessing cleaning quality. INSTA 800 is a joint Nordic cleaning standard. NS-INSTA 800 entails 5 different quality levels, where 5 is the highest and 1 is the lowest. The quality levels are determined based on the size of the room, the set quality level for the individual surfaces in the room, and whether the surfaces are easily accessible or difficult to reach. The standard assumes that the quality levels must be quality assured at least 4 times each year. Dust cover percentage is used to measure how much waste, dirt, dust, and stains there is per $cm^2$ and is used in connection with the control of cleaning of surfaces, including in ventilation systems. The standard distinguishes between whether the location of the dirt is easily accessible or not. More dirt is allowed in hard-to-reach places [12].

## 2.3 Deposition of Particulate Matter

Several studies have looked at the particle deposition rates for varying particle sizes, a study done in Australia looked at different studies and compared the results [13], all of the reviewed studies were done on residential houses. The deposition rates found from the different studies can be viewed in figure 2.1.

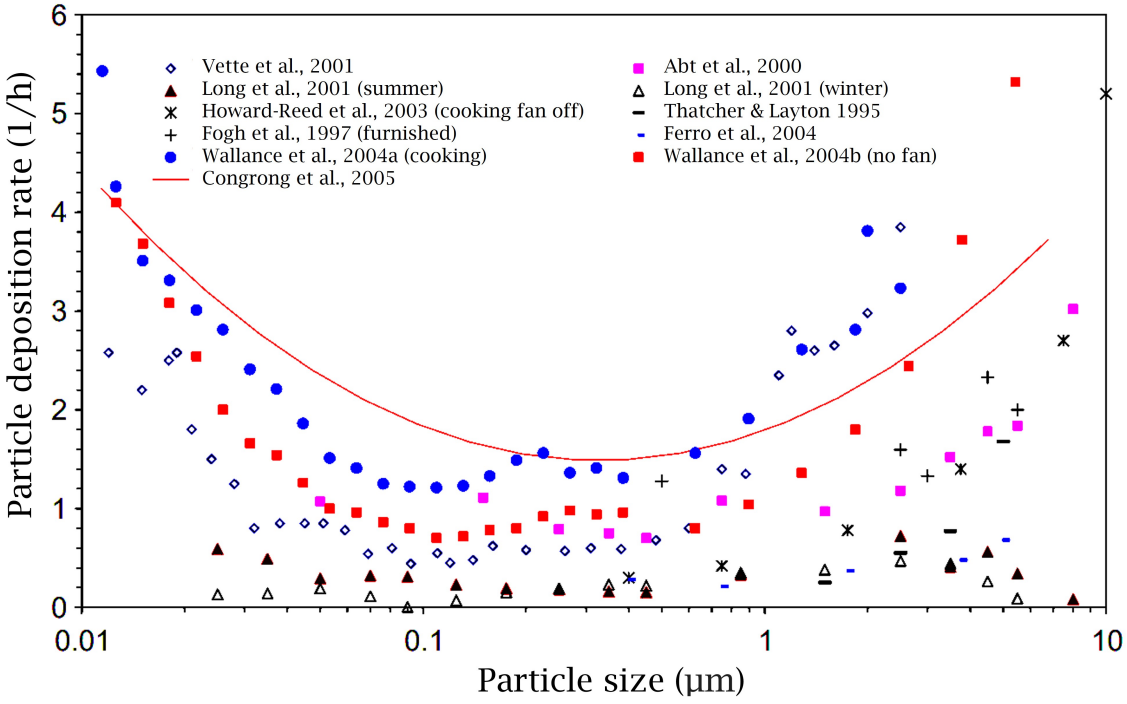


Figure 2.1: Comparison of particle deposition rates reported in literature [13].

The deposition rates of particles vary depending on their size and ventilation conditions. Research has shown that particles in the range of 0.2 to 0.3 µm exhibit the lowest deposi-

tion rates. Statistical analysis revealed that the air exchange rate significantly influences deposition rates for particles sized between 0.08 and 1.0 µm, but not for particles smaller than 0.08 µm or larger than 1.0 µm [13].

Transitioning from a bare surface to a fully furnished one led to an increase in deposition loss rates, particularly notable for smaller particles. Additionally, elevating the mean airspeed resulted in higher deposition rates across all particle sizes, with larger particles experiencing more pronounced effects than their smaller counterparts [14].

### 2.3.1 Gravitational Settling

Gravitational settling is a process by which particulate matter in a fluid falls to the bottom due to the force of gravity.

Larger and denser particles settle more quickly than smaller and less dense particles because they experience a greater gravitational force relative to their resistance to falling (drag force). The terminal velocity of a particle, which is the constant speed it eventually reaches when the gravitational force is balanced by the drag force, is higher for larger and denser particles. The gravitational force ($F_g$) acting on a particle is given by $F_g = m \cdot g$, where $m$ is the mass of the particle and $g$ is the acceleration due to gravity (approximately 9.81 m/s$^2$ on Earth).

As a particle falls through a fluid, it experiences a drag force ($F_d$) opposing its motion. The drag force depends on factors such as the particle's velocity, the fluid's viscosity, and the particle's shape and size. For small spherical particles, the drag force can be described by Stokes' Law: $F_d = 6\pi\eta r v$, where $\eta$ is the dynamic viscosity of the fluid, $r$ is the radius of the particle, and $v$ is the velocity of the particle. The terminal velocity ($v_t$) is reached when the gravitational force equals the drag force, resulting in zero net acceleration.

The viscosity and density of the fluid through which particles are settling significantly affect the settling velocity. Higher viscosity fluids slow down the settling process. The shape, size, and density of particles influence their settling behavior. Irregularly shaped particles experience different drag forces compared to spherical particles.

### 2.3.2 Ventilation Effect

Ventilation plays a crucial role in determining particulate matter values in indoor environments. Effective ventilation systems can significantly reduce PM concentrations by introducing fresh outdoor air and diluting indoor pollutants [15]. Proper ventilation helps remove particulate matter generated by indoor activities as well as biological particles like dust mites and pet dander. Several studies have proven that indoor particulate matter values are significantly influenced by indoor activities and that indoor PM levels can exceed outdoor levels quite quickly [16, 17].

Inadequate ventilation can lead to higher PM levels, as pollutants accumulate and recirculate within the space. This can worsen indoor air quality and pose health risks,

particularly for vulnerable populations such as children, the elderly, and those with respiratory conditions [2, 5]. Higher PM levels also result in higher deposition rates of particles on indoor surfaces, which can further contribute to health issues and necessitate more frequent cleaning and maintenance. Advanced ventilation systems equipped with high-efficiency particulate air (HEPA) filters are particularly effective in capturing fine particles, further improving air quality and reducing exposure to harmful pollutants [18].

## 2.4 Resuspension of Particulate Matter

The resuspension of particulate matter is a phenomenon that involves the re-entry of particles into the air after they have initially settled or deposited onto various surfaces. Resuspension is caused by changes in air movement that disturb the settled particles and causes them to become airborne again. The changes in the air can be caused by human activity, natural sources such as wind or mechanical systems, such as HVAC systems. The circulation of air within buildings can disturb settled particles and reintroduce them into the air.

### 2.4.1 Ambient Temperature and Relative Humidity

Changes in ambient temperature and relative humidity (RH) significantly impact the suspension and deposition of particulate matter [19]. The deposition of fine PM is influenced by thermophoretic forces resulting from temperature gradients. Additionally, RH plays a crucial role, affecting the adhesion force between particles in a non-linear manner [20].

Under high RH conditions, the contribution of van der Waals attractive forces diminishes, and adhesion is predominantly governed by capillary forces. Extra water on surfaces enhances capillary forces by creating meniscuses between particles and surface asperities [21]. This leads to capillary coagulation between particles, increasing surface adhesion and inhibiting resuspension [22].

Conversely, as temperature increases and RH decreases, adhesive forces between particles and surfaces weaken, elevating the rate of resuspension [23]. Studies by Corn and Stein indicated that adhesion forces remain constant up to an RH of 30%, after which they increase rapidly [20]. This underscores the intricate interplay between temperature, RH, and the various forces governing particle deposition and resuspension in ambient conditions.

### 2.4.2 Air Velocity and Turbulence

When the speed of air close to a surface increases, the hydrodynamic force on a particle also rises. This implies that higher overall airflow velocity can cause the flow to become turbulent. Particles on a surface experience various stresses within the viscous sublayer of this turbulent boundary layer. Consequently, a steady force from the fluid opposes the adhesive force keeping the particle on the surface. According to the quasi-static model, when the airflow reaches a certain speed, the hydrodynamic forces surpass the adhesive

forces, causing the particle to be promptly lifted off, resulting in immediate resuspension [24].

Even though the air drag force near the boundary layer might be minimal, the drag force on particles in the free stream significantly outweighs gravity. When particles move through the boundary layer into the stronger free stream, the intense drag can keep them suspended for a longer period [20, 25].

## 2.5 Methods for Measuring Particulate Matter

Particulate matter comes from various sources. In urban areas, vehicle emissions, including fine particles from exhaust, tire, and brake wear, are significant contributors [26]. Industrial processes, such as manufacturing and power plants, release both primary particulates, directly emitted, and secondary particulates, formed through chemical reactions involving gases like sulfur dioxide and nitrogen oxides [27]. Agricultural activities, including tilling, harvesting, and large feedlots, release dust, soil particles, and particulates from animal waste and feed [28]. Residential activities, such as using wood-burning stoves and fireplaces, may also increase localized particulate pollution [29].

Particulate matter can also come from human bodies, shedding substances from skin, hair, and clothing, known as "bioaerosols," affecting indoor and sometimes outdoor air quality [30]. Depending on the type of particulate matter being sampled and the specific requirements of the analysis, different sampling methods are employed.

### 2.5.1 Bulk Sampling

**Vacuum cleaners**
Vacuum cleaners equipped with HEPA filters and specialized collection bags are effective tools for dust sampling. This method involves systematically moving the vacuum nozzle over surfaces to collect dust. It's suitable for comprehensive assessments of indoor air quality and surface cleanliness, allowing the collection of significant dust quantities from carpets, upholstery, and other surfaces. The method's effectiveness depends on the vacuum's filtration efficiency and the thoroughness of the sampling process, enabling the analysis of various contaminants, including allergens, microbial spores, and particulate matter [31].

**Brooms and brushes**
Brooms and brushes are simple and effective tools for dust collection, especially from floors, walls, and surfaces that vacuums might not reach. This method doesn't require electricity, making it ideal for areas sensitive to electrical interference. It is adaptable to various surface types and contamination levels, with customizable techniques and types of brooms or brushes to meet specific needs [32].

### 2.5.2 Passive Sampling

**Settled Dust Boxes**
Settled dust boxes are simple yet effective passive sampling devices. They consist of a container with an open top that houses a collection surface. Placed in strategic locations, they allow dust to settle naturally over time. Their design minimizes disturbance from air currents or human activity, preventing external contamination. After the collection period, the box is sealed, and the dust is retrieved for analysis. This method is useful for evaluating dust deposition rates and associated contaminants, providing insights into long-term particulate matter accumulation in indoor environments [33].

**Dust Trap**
Dust traps passively collect airborne particles through filtration and gravitational settling mechanisms. Air flows through an enclosed space where particles settle on sticky surfaces or within a containment area. Dust traps can be customized to target specific particle sizes and types, making them versatile for monitoring indoor air quality. They are ideal for continuous or long-term studies, operating unobtrusively without active intervention. The data collected informs on the dynamics of airborne particulate matter, including trends over time and responses to changes in the indoor environment [34].

### 2.5.3 Manual Sampling

**Dust Tape**
Dust tape sampling is an efficient method for collecting dust from hard surfaces. Clear adhesive tape is pressed against surfaces like floors, walls, windowsills, and furniture to lift dust particles. The tape, with dust particles attached, is then placed on a slide for microscopic analysis or chemical testing [35].

**Foil Sampling**
Foil sampling involves using sticky gelatin foil to collect surface contamination. The amount of dust, or dust index, is determined by analyzing light scattered across the foil. This method quantifies the percentage of the area covered by dust and is noted for its reproducibility and ease of use, detecting dust-covered areas of less than 0.1% [36].

### 2.5.4 Gravimetric Method

The gravimetric method measures the concentration of particulate matter in the air by weighing collected particles. Air containing particulate matter is drawn through a filter or onto a collection surface for a specific period, typically 24 hours or more. After the collection period, the filter is carefully removed and weighed. The increase in weight corresponds to the mass of the collected dust particles, and this concentration is expressed as mass per unit volume [37]. This method is simple and cost-effective, making it suitable for various types of particulate matter. However, it is time-consuming, as results are not available immediately, and it may not capture rapid changes in dust concentrations. Additionally, it is susceptible to errors due to handling and potential contamination.

### 2.5.5 Light Scattering Method

Particulate matter sensors are categorized into two types based on laser and infrared principles, both employed for detecting airborne particles and monitoring indoor air quality to alert against pollution.

**Infrared Sensor** The infrared-based PM sensor features a straightforward structure, utilizing an infrared light-emitting diode (LED) as its source. Operating on the principle of light scattering, the LED emits light that encounters particles, causing reflection. The photosensitive element gauges the intensity of the reflected light, determining particle concentration based on pulse signal intensity through processing and classification algorithms. When no particles are detected, the photosensitive detector outputs a low pulse; conversely, when particles are detected, the output is a high pulse [38].

**Laser Sensor** The laser particle sensor uses a laser scattering-based optical particle counter to quickly provide the PM concentration in the environment. With a laser LED as the light source, the structure and circuit of the laser PM sensor are more intricate than those of the infrared sensor. As fine particles or dust in the air enter the sensor's laser beam, the laser light scatters. A photodetector positioned to receive only scattered light generates an electrical signal through the photoelectric effect. After amplification by the circuit, the concentration of fine particles can be determined [38].

# 3 Theoretical Basis

## 3.1 Particle Deposition Models

Particle deposition models are mathematical or computational representations that describe the process of particles settling or depositing on surfaces. Different models may focus on specific aspects of particle deposition, taking into account factors such as particle size, surface characteristics, airflow patterns, and environmental conditions.

### 3.1.1 Inertial Impaction Models

Inertial impaction models describe the deposition of airborne particles on surfaces due to their inertia when influenced by changes in airflow direction. These models are particularly relevant when particles are carried by a gas or fluid stream with varying velocities and directions. Inertial impaction becomes a dominant mechanism for larger particles when the airflow changes direction, causing the particles to impact and deposit on surfaces [39].

The basic principle behind inertial impaction is that particles in motion have momentum. When the airflow changes direction, such as around a bend or in a curved duct, the particles tend to continue in a straight path due to their inertia. Consequently, larger and heavier particles may impact and deposit on surfaces, while smaller particles may follow the curving airflow more closely.

Inertial impaction models often consider factors such as particle size, airflow velocity, and the curvature of the flow path. One commonly used equation in inertial impaction modeling is the Stokes number, a dimensionless parameter representing the ratio of particle inertia to viscous forces in the fluid. The Stokes number is often used to predict the behavior of particles in changing flow conditions [40].

### 3.1.2 Particle Motion in a Fluid Medium

When a particle navigates through a continuous fluid medium, its acceleration is impacted by the difference in velocity between the particle and the fluid, as well as the pressure exerted on both the particle and the fluid due to external forces. This particle movement can be described by Newton's second law of motion, as indicated in Equation 1 [41].

$$m_p \frac{du_p}{dt} = \underbrace{3\pi \mu d_p (u_f - u_p)}_{\text{I}} + \underbrace{\frac{\pi d_p^3 \rho_f}{6} \frac{du_f}{dt}}_{\text{II}} + \underbrace{\frac{\pi d^3 \rho_f}{12} (\frac{du_f}{dt} \frac{du_p}{dt})}_{\text{III}} + \underbrace{\frac{3}{2} d_p^3 \sqrt{\pi \rho_f \mu} \int_{t_0}^{t} \frac{\frac{d_p u_f}{dt'} - \frac{du_p}{dt'}}{\sqrt{t - t'}} dt'}_{\text{IV}} + \underbrace{Fe}_{\text{V}} \quad (1)$$

The acceleration of the particle, shown on the left side of the equation, equals the sum of all forces acting on the particle. The first term, labeled I, represents the viscous drag exerted by the fluid over the particle's surface according to Stokes' law. The second term, II, is the force acting on the particle due to the pressure gradient within the surrounding fluid caused by fluid acceleration. The third term, III, pertains to the force needed to accelerate the virtual mass of the fluid that occupies the particle's volume, especially significant when the displaced fluid's mass exceeds that of the particle. The fourth term, IV, known as the Basset force or history term, accounts for changes in the flow pattern from steady state, increasing the instantaneous flow resistance when the particle undergoes rapid acceleration due to an external force. The fifth term, V, includes any external forces directly affecting the particle, such as gravitational or electrical forces.

When the fluid density is less than the particle density, the second, third, and fourth terms become negligible. In such cases, the equation simplifies to Equation 2 [41].

$$\frac{\pi d_p^3 \rho P}{6} \frac{du_p}{dt} = 3\pi v \mu d_p \frac{X}{C_c} (u_f - u_p) + Fe \quad (2)$$

The particle's acceleration is influenced by the immediate velocity difference between the particle ($u_p$) and the gas ($u_f$), and the external body force ($F_e$). To address experimental observations on the viscous drag of a solid sphere, the slip correction factor ($C_c$) is used. Additionally, Stokes' law is adjusted with the dynamic shape factor ($\chi$) to account for the effect of particle shape on drag [41].

## 3.2 Particulate Matter Balance

### 3.2.1 Indoor – Outdoor Environment Exchange

To calculate the concentration of aerosol particles within an indoor environment, consideration of various factors influencing particle dynamics is essential. These factors include the volume of the room ($V$), the outdoor ($C_{\text{ext}}$) and indoor ($C_i$) concentrations of aerosol particles, the rate of deposition ($\lambda_{\text{de}}$) of particles onto surfaces, the resuspension rate ($\lambda_R$) of particles from surfaces back into the air, the infiltration coefficient ($f$) representing the efficiency of outdoor particles penetrating indoors, the rate of penetration ($\lambda_p$) of particles from the exterior to the interior, the concentration of resuspended particles ($C_{Di}$), and the strength of indoor particle sources ($S_i$). The overall concentration of aerosol particles as a function of time (t) is expressed in equation 3 [42].

$$\frac{dC_i}{dt} = f\lambda_p C_{ext} - \lambda_p C_i - \lambda_{de} C_i + \lambda_R C_{Di} + S_i \tag{3}$$

Indoor aerosol particle concentrations are affected by external air quality, human activity, ventilation systems, and the physical and chemical transformations particles experience indoors. Both the deposition rate, which describes how particles settle on surfaces, and the resuspension rate, which details how these particles are reintroduced into the air, are vital for understanding indoor air quality. The penetration factor measures the efficiency with which outdoor aerosol particles enter an indoor space through openings or ventilation systems, and is influenced by the building's design and the operation of heating, ventilation, and air conditioning systems, as well as the effectiveness of air filters. The rate of penetration specifically addresses the movement of particles from outside to inside, shaped by air exchange rates and air filtration systems. The concentration of resuspended particles depends on the rate at which particles are lifted from surfaces into the air, which is affected by human activities, airflow patterns, and surface characteristics within the room. Finally, internal sources of particles, such as cooking, smoking, consumer product usage, and mechanical processes, significantly impact the overall concentration of indoor aerosol particles.

### 3.2.2 Particulate Matter Deposition

The deposition of particulate matter ($D_e$) is intricate and influenced by various factors such as air velocity, humidity, and electrostatic forces. However, simplified models are used to simulate the rate at which particulate matter deposits [42].

Equation 4 expresses how particulate matter deposition can be calculated using the rate of deposition ($\lambda_{de}$) and the indoor concentration of particulate matter ($C_i$).

$$D_e = \lambda_{de} \cdot C_i \tag{4}$$

The rate of deposition can be obtained using Equation 5, where $S$ is the surface area, $V$ is the volume of the room, and $V_d$ is the speed of deposition [42].

$$\lambda_{de} = \frac{S}{V} \cdot V_d \tag{5}$$

The speed of deposition can be found using the flow density (J) and the indoor concentration of particulate matter ($C_i$), as seen in Equation 6 [42].

$$V_d = \frac{J}{C_i} \tag{6}$$

### 3.2.3 Particulate Matter Resuspension

Resuspension refers to the process by which particles that have previously settled onto surfaces are reintroduced into the air. This phenomenon plays a significant role in determining the concentration of particles within an indoor environment. Factors influencing resuspension include human activities, such as walking or cleaning, as well as air currents and other mechanical disturbances. Calculating the resuspension rate of aerosol particles ($\lambda_R$) presents several challenges due to the complexity of the factors involved and the variability of conditions under which resuspension occurs.

Due to the difficulties separating resuspension and deposition equation 7 is often assumed [42], where ($\lambda_d$) is the combination of the resuspension rate and the deposition rate.

$$Ci\lambda_d \approx C_i\lambda_{de} + C_{di}\lambda_R \tag{7}$$

This leads to equation 3 being simplified into equation 8.

$$\frac{dC_i}{dt} = f\lambda_p C_{ext} - \lambda_p C_i - \lambda_d C_i + S_i \tag{8}$$

When integrated, equation 8 results in equation 9, representing a time-dependent solution for the indoor concentration of particulate matter.

$$C_i(t) = C_{ext} \cdot \frac{\lambda_p}{\lambda_p + \lambda_d}(1 - e^{-(\lambda_p+\lambda_d)t} + C_i(0) \cdot e^{-(\lambda_p+\lambda_d)t} + S_i(t)) \tag{9}$$

# 4 Methodology

The central focus of the research question is to quantify and describe the correlation between airborne particles and their deposition in Norwegian schools.

To answer this question, large amounts of data are needed, encompassing both the indoor environment and the rate at which dust deposition occurs. The following chapter elaborates on the equipment, data-collection methods, locations, and processing methods employed to quantify the data and obtain reliable results.

## 4.1 Outline of Method

A visual outline of the method can be viewed in figure 4.1.

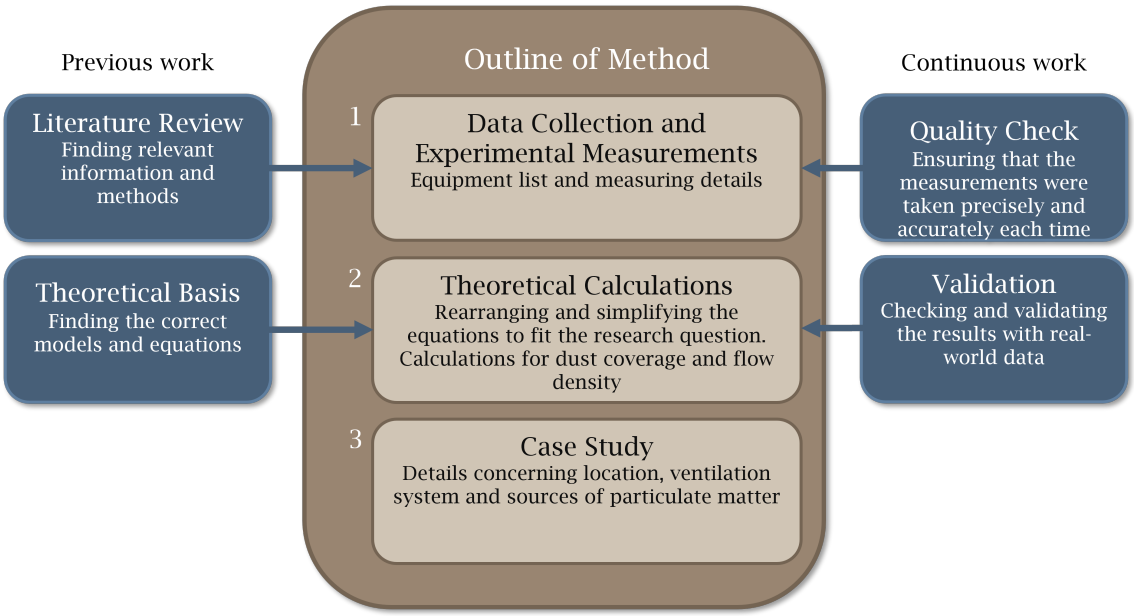


Figure 4.1: Visual outline of method

## 4.2 Data Collection and Experimental Measurements

This section details the methodologies employed for data collection and the experimental measurements pivotal to the study. Accurate and reliable data are essential for understanding dust deposition rates and particulate matter behavior. By detailing the procedures, equipment, and conditions under which data were gathered, this section provides a comprehensive overview of the experimental framework. This foundation ensures the validity of the findings and allows for reproducibility in future studies.

### 4.2.1 Empirical Analysis and Quantitative Research

This research uses a grounded, empirical approach focusing on an evidence-based method for analyzing and interpreting data. It prioritizes real-world data and outcomes over abstract theories, ensuring conclusions are backed by observable evidence. Data collection involves environmental sensors and manual sampling, essential for obtaining accurate data. The environmental sensors provide quantifiable digital data, while manual sampling allows for physical data verification. The data's reliability is highlighted by its consistency and the ability to corroborate with previous research, enhancing credibility and contributing to the field's knowledge base.

### 4.2.2 Equipment

The equipment used for the measurements can be viewed in table 4.1.

Table 4.1: Equipment

| **Equipment name** | **Information** |
|---|---|
| BM Dust Detector | Measures dust percentage coverage |
| NSIAQ Environmental Sensor | Measures $CO_2$, temperature, PM10, PM2.5 and RH |
| VelociCalc TSI | Measures air velocity |
| Collection plate | Collection plate for dust percentage coverage measurements |

**BM Dust Detector** During dust measurement with the BM Dust Detector, dust deposits are registered on a special gel foil. The foil is illuminated before and after sampling, and the change in the amount of light (reduced due to dust) is a direct measure of the amount of dust deposited on the foil. The dust quantity is directly read in percentage, and the result indicates how many percent of the tape is covered with dust. Measurement of the dust coverage can provide information about both the pollution level in the specific room and the effectiveness of different cleaning methods.

**Environmental Sensor** The Environmental Sensor is an Internet of Things (IoT) device designed for environmental measurements. It is a laser sensor and includes a range of sensors to capture key data points within buildings. The device is capable of monitoring temperature, humidity, $CO_2$ concentration, and airborne particulate matter, transmitting data using Long-Term Evolution Narrowband IoT technology. While it is equipped with an embedded Li-Ion battery to address mains power interruptions, its primary design is intended for connection to the mains network. The sensors are located at approx. 1.50 -1.70 [m] above floor level and are situated away from windows and doors to eliminate disturbances to the measurements caused by increased air velocity and direct sunlight.

The accuracy and range of the sensor can be viewed in table 4.2

Table 4.2: NSIAQ Environment Sensor accuracy and range

| Parameter | Accuracy | Range |
|---|---|---|
| Temperature | ± 0.2[°C] | –40 to 125[°C] |
| Relative Humidity | ± 2[%] | 0 to 100[%] |
| $CO_2$ Consentration | ± 50 ppm + 5% of reading | 400 to 2000 [ppm] |
| Particulate Matter | not given | ≤ 10 (µm) (Particle size) |

#### VelociCalc TSI

the velocicalc TSI is a measuring device used to measure air velocity and temperature, and calculate volumetric flow rates. The device can store individual readings and compute averages of these readings

#### Collection Plate

The collection plate consisted of a small shelf measuring 21.0cm x 29.7cm (A4 size) with a removable birch plate covering the top surface. The shelf was placed above the reach of the children in the classroom to avoid contamination of the measurements, approximately 2.2 meters above the floor. The collection plates was always mounted to the same wall as the environmental sensors to ensure reliable comparability with the airborne measurements. Each classroom had two collection plates, one for each testing day as to not contaminate the measurements with increased air velocity during the measuring with the BM dust detector.

### 4.2.3 Measuring Details

The measurements were taken at 48-hour intervals. The collection plate was cleaned every Monday and then tested for dust percentage cover on Wednesdays and Fridays. When using the BM Dust Detector, three samples were taken each time to ensure reliable results. The gel tapes for testing were evenly distributed on the collection plate with an approximate distance of 3 cm between each tape. The testing period lasted three weeks, with a one-week break in the middle due to the school being closed for the winter break. The dates of the testing weeks can be viewed in Table 4.3. The measurements were always taken in the morning, at 8 AM, before the children arrived at school.

Table 4.3: Testing periods details

| | Start date | End date |
|---|---|---|
| **Week 1** | 19.02.2024 | 23.02.2024 |
| **Week 2** | 04.03.2024 | 08.03.2024 |
| **Week 2** | 11.03.2024 | 15.03.2024 |

## 4.3 Theoretical Calculations

### 4.3.1 Averaging and Defining the Measurements

Three samples were taken for each measurement with the BM dust detector to ensure reliable results. The samples were averaged and the sample variance for the measurements were found using equation 10. Where $\sigma^2$ is the sample variance, $x_i$ is the value of one sample, $\overline{x}$ is the mean value of all the samples and $n$ is the number of samples.

$$\sigma^2 = \frac{\sum(x_i - \overline{x})^2}{n-1} \tag{10}$$

The data from the IAQ sensors were analyzed to determine the share of PM2.5 in the total PM10. This was achieved by simply dividing the PM2.5 data by the PM10 data for the selected time period.

### 4.3.2 Dust Coverage Calculations

The variation in dust load over time is described as the net result of particles depositing onto the surface minus the particles which are resuspended from the surface [41].

By utilizing equations 4 and 7, an expression for the settled dust load ($\phi$) is presented, as shown in equation 11. The resuspension is assumed to be proportional to the dust load on the surface [43].

$$\frac{d\phi}{dt} = \underbrace{V_d Ci}_{Deposited} - \underbrace{\lambda_R \phi}_{Resuspended} \tag{11}$$

Equation 11 is solved with the assumption that the speed of deposition ($V_d$) and the rate of resuspension ($\lambda_R$) remain constant. This leads to Equation 12, which illustrates how the amount of settled dust changes over time, considering both deposition and resuspension processes.

$$\phi(t) = \left(\phi_0 + V_d \int Ci(t) e^{\lambda_R t}, dt\right) e^{-\lambda_R t} \tag{12}$$

Due to the collection method of deposited particles, there is no way to separate the deposition rate from the resuspension rate. The combined deposition and resuspension rate ($\lambda_d$) is assumed according to equation 7. This simplifies equation 12 to equation 13.

$$\phi(t) = \phi_0 + \lambda_d \int Ci(t), dt \tag{13}$$

### 4.3.3 Flow Density Calculations

The rate of deposition can be calculated using Equation 5. However, the flow density ($J$) is unknown. To determine the flow density using the dust coverage percentage, Equation 14 was created. $J$ was calculated using the cross-sectional area of the particles ($A_p$), Dust coverage percentage ($D_c$), collection time ($t$), and mass of the particles ($m_p$).

$$J = \frac{D_c}{A_p \cdot t} \cdot m_p \tag{14}$$

Assuming the particles distribute uniformly across the surface, the probability ($p$) of a new particle landing on another particle is directly proportional to the fraction of the surface covered by particles. Therefore, $p$ can be expressed simply as the fraction of the surface covered, or the dust load ($D_c$), assuming uniform coverage and no effects of particle size or other complicating factors. Essentially, this approach assumes each spot on the surface is equally likely to receive the next particle, as shown in Equation 15.

$$p = D_c \tag{15}$$

Given this probability, the flow density can be rewritten as shown in Equation 16. Here, the probability of particles landing on top of each other is accounted for using the median dust load $\left(\frac{D_c}{2}\right)$.

$$J = \frac{(1 + \frac{D_c}{2}) \cdot D_c}{A_p \cdot t} \cdot m_p \tag{16}$$

The mass of the particle ($m_p$) was assumed based previous research, where the mass of particulate matter was set to 1500 kg/$m^3$ [44]. Assuming the particles are spherical, the cross-sectional area of each particle ($A_p$) was calculated based on the average particle diameter. The average particle diameter was determined using the particulate matter values from the IAQ sensors and Equation 17. In this context, $1.25\mu m$ represents the average diameter of a particle 2.5 $\mu m$ or smaller, while $3.75\mu m$ is the average diameter of a particle between 2.5 $\mu m$ and 10 $\mu m$.

$$\text{Particle diameter} = \frac{\text{sum of PM2.5}}{\text{sum of PM10}} \cdot 1.25\mu m + (1 - \frac{\text{sum of PM2.5}}{\text{sum of PM10}}) \cdot 3.75\mu m \tag{17}$$

## 4.4 Case Study - Lundstein Primary School

Lundstein Primary School is a primary school in Gjøvik, approximately six kilometers north of the city center. The school is dimensioned for 80 students and opened in 2012. The school can be viewed in figure 4.2.


Figure 4.2: Lundstein Primary School [45]

### 4.4.1 Room Description

Four rooms were chosen for examination: three classrooms and one common room. The locations of these rooms within the building can be viewed in Figure 4.3. Rooms 1, 2, and 3 are classrooms, while Room 4 is the common room. The dotted lines in the rooms represent divider walls that are open part of the time. Students use the entrances on the south side of the building, while employees use the main entrance.

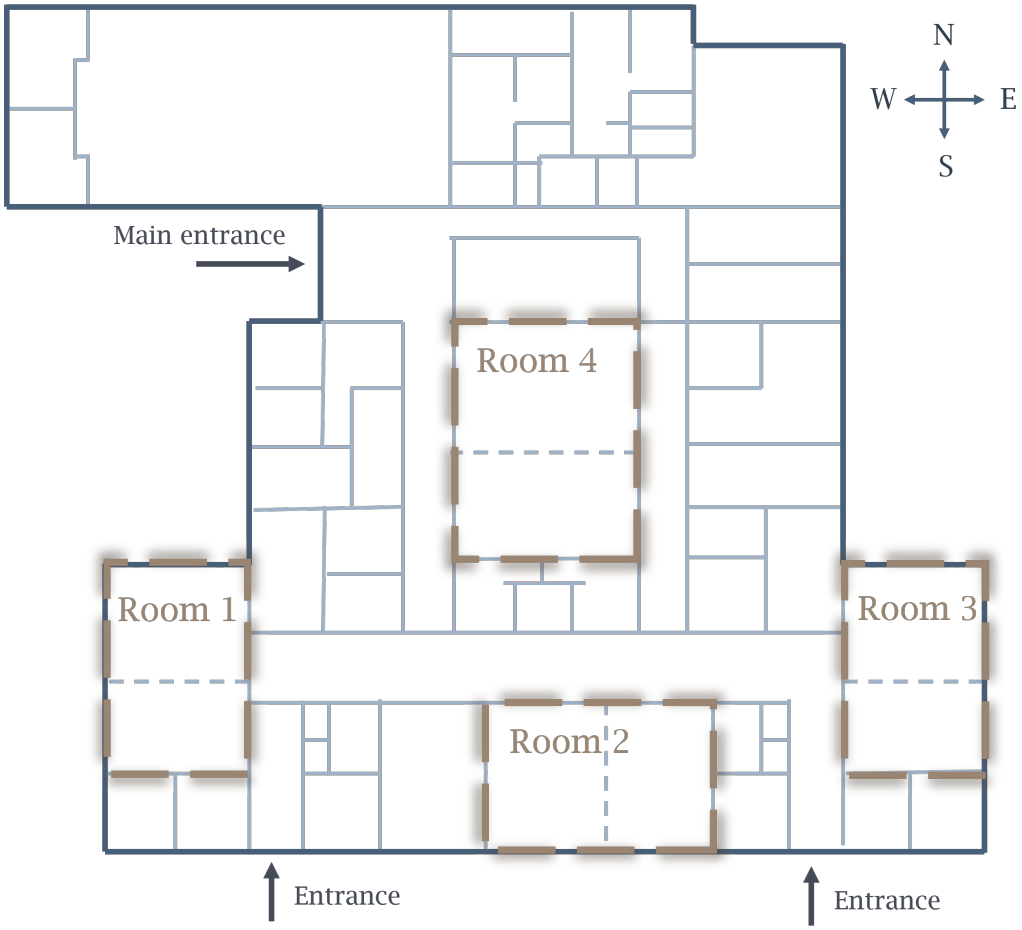


Figure 4.3: Floorplan and chosen rooms

The specification of the rooms can be viewed in table 4.4.

Table 4.4: Specification of the rooms

| **Room** | **Area** $[m^2]$ | **Volume** $[m^3]$ | **Intake vents** | **Extract vents** |
|---|---|---|---|---|
| Room 1 | 65.5 | 163.75 | 5 | 2 |
| Room 2 | 73.6 | 184 | 5 | 2 |
| Room 3 | 65.5 | 163.75 | 5 | 2 |
| Room 4 | 105.3 | 421.2 | 6 | 0 |

### 4.4.2 Ventilation system

The ventilation system at Lundstein Primary School comprises two circuits, with ducts leading to individual classrooms. All the investigated rooms are on the same circuit. It operates mechanically, featuring vents in the ceiling for both fresh and used air, employing mixed ventilation. The system has variable air volume (VAV) and is regulated based on the $CO_2$ levels in the rooms. While the set point for increased air volume is adjustable,

it remains fixed at 500ppm $CO_2$ during the examined period. The set point temperature is set to 20 °C. The vents supplying fresh air has a max capacity of 282 $m^3/h$ each.

The air intake is positioned on the wall of the technical building, away from the schoolyard, while the air exhaust is situated on the roof of the same building , both visible in Figure 4.4. The fans have a maximum capacity of 16400 $m^3/h$, and during regular operation, they typically operate at about half capacity. There is one fan dedicated to the air intake and another for the exhaust. The system incorporates a rotary heat exchanger.

The system follows a predefined schedule and operates solely between 06:30 and 16:30 on weekdays. Beyond these operating hours, as well as during weekends and vacations, the system remains inactive. However, if the building is utilized outside the designated operating hours, a manual dial allows users to activate the system for a specified duration.

Figure 4.4: Air intake and exhaust

The ventilation system employs glass fiber bag filters with plastic frames, adhering to the ISO16890 standard. Specifically, the Hi-Flo XLT 7/640 0160 filter is utilized for both the air intake and exhaust. Filter replacement is scheduled annually, with the most recent replacement dated 09.11.2023.

The key parameters of the ventilation system can be viewed in tables 4.5 and 4.6.

Table 4.5: Ventilation specifications

| Parameter | Specification |
|---|---|
| Filter | Hi-Flo XLT 7/640 0160 |
| System | Mechanical |
| Air flow | VAV |
| Air distribution | Mixed ventilation |
| Operating hours | Weekdays 0630 - 1630 |

Table 4.6: Ventilation parameters

| Parameter | Value | Unit |
|---|---|---|
| Fan capacity | 16400 | $m^3/h$ |
| Vent capacity | 382 | $m^3/h$ |
| Setpoint temp | 20 | °C |
| Setpoint $CO_2$ | 500 | ppm |
| Setpoint pressure | 170 | Pa |

### 4.4.3 Sources of Particulate matter

The school had multiple potential sources of particulate matter. Cooking in the school kitchen released particles from food preparation. Human activities, such as movement and interaction, also contributed to indoor particulate levels. Outdoor play areas were significant sources, with particles coming from sand, gravel, snow, and nearby road pollution. Additionally, particulate matter could be tracked into the school on clothes and shoes from various external environments. Children entered the building through entrances that opened directly onto the paved part of the schoolyard, which also included grass and sand areas. During the measurements, the pavement was mostly covered in snow and ice. To reduce debris and moisture entering the building, metal scraper mats were placed outside the entrances and absorbent scraper mats inside. Inside, the hallway between the classrooms functioned as a locker room for storing outdoor shoes and clothes.

Given that the measurements were conducted in winter and early spring, the likelihood of pollen and other organic sources was low.

# 5 Results

This section outlines the results of the dust percentage measurements, IAQ data captured through sensors, and calculated findings. Key data and results are organized in tables and figures to enable straightforward comparisons across the different testing locations.

## 5.1 Results from Data Collection and Measurements

The first section presents the dust percentage measurements obtained using the BM Dust Detector and the IAQ data obtained using the environmental sensors.

### 5.1.1 Foil Measurements

The dust percentage measurements taken with the BM Dust Detector showed varying results. The average of the samples for each measurement can be viewed in table 5.1. The variation between each of the three samples done for each measurement showed a large variance, the variance between the samples can be viewed in table 5.2. For all of the measurements, view appendix A.

Table 5.1: Average dust coverage percentages

| | **Date** | **Room 1** | **Room 2** | **Room 3** | **Room 4** |
|---|---|---|---|---|---|
| Week 1 | Wednesday 21.02 | 3.3 | 2.9 | 2.9 | 3.3 |
| | Friday 23.02 | 3.0 | 2.9 | 3.6 | 4.4 |
| Week 2 | Wednesday 06.03 | 1.5 | 1.7 | 1.8 | 1.3 |
| | Friday 08.03 | 3.3 | 1.5 | 2.5 | 1.6 |
| Week 3 | Wednesday 13.03 | 3.4 | 2.9 | 3.5 | 2.7 |
| | Friday 15.03 | 2.0 | 2.3 | 4.1 | 3.5 |

Table 5.2: Variance in measurements

| | **Date** | **Room 1** | **Room 2** | **Room 3** | **Room 4** |
|---|---|---|---|---|---|
| Week 1 | Wednesday 21.02 | 1.5 | 1.0 | 2.0 | 7.9 |
| | Friday 23.02 | 4.0 | 0.5 | 4.9 | 0.9 |
| Week 2 | Wednesday 06.03 | 1.2 | 0.6 | 0.3 | 0.0 |
| | Friday 08.03 | 1.7 | 0.1 | 0.2 | 0.2 |
| Week 3 | Wednesday 13.03 | 3.4 | 0.3 | 1.4 | 0.0 |
| | Friday 15.03 | 0.4 | 1.2 | 0.2 | 0.8 |

### 5.1.2 Data From Sensors

To accurately estimate the size of particulate matter particles, needed to calculate the rate of deposition, the PM2.5 data needed to be separated from the PM10 data. PM2.5 represented more than 80% of the particulate matter in all instances, except for the measurements in Room 2, which showed a notably lower PM2.5 proportion. The results detailing the PM2.5 share of total particulate matter are presented in Table 5.3, the codes used for the calculations can be viewed in appendix B.1.

Table 5.3: PM2.5 share of total particulate matter

| | **Intervall** | **Room 1** | **Room 2** | **Room 3** | **Room 4** |
|---|---|---|---|---|---|
| Week 1 | 19.02-23.02 | 96% | 14% | 87% | 96% |
| Week 2 | 04.03-08.03 | - | 28% | 90% | 97% |
| Week 3 | 11.03-15.03 | 94% | 16% | 84% | 94% |

The sensor in room 1 was down for parts of week 2 and the data could not be used due to being incomplete.

The difference between the particulate matter share between room 1 and 2 in week 1 can be viewed in figure 5.1 and 5.2. Room 1 has a notable higher share of PM2.5 than room 2.

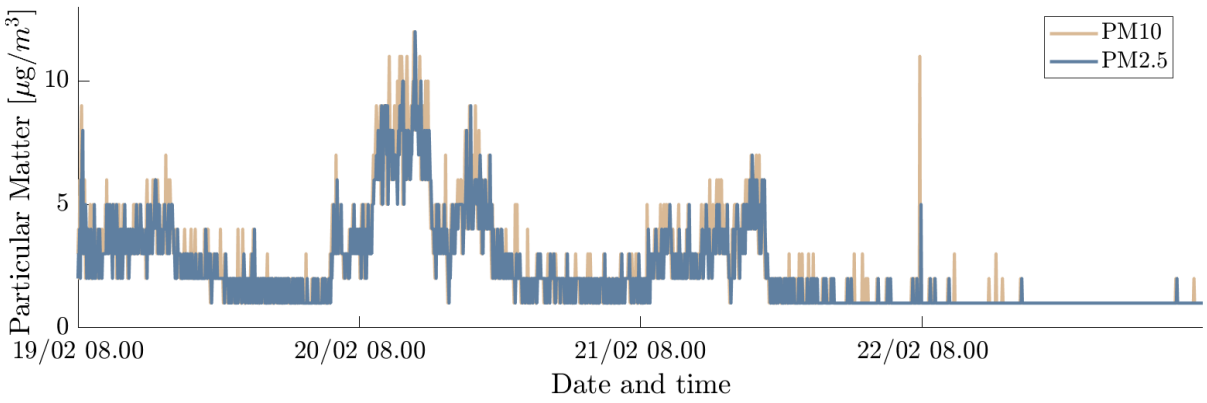


Figure 5.1: PM10 and PM2.5 in room 1, week 1

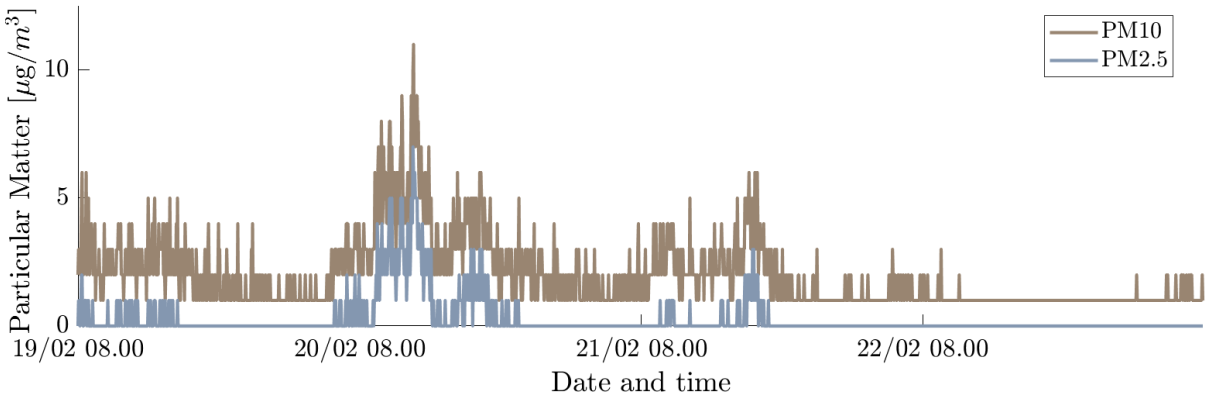


Figure 5.2: PM10 and PM2.5 in room 2, week 1

## 5.2 Results From Theoretical Calculations

This section provides an analysis of the calculated rate of deposition over various time intervals, using data from dust measurements and environmental sensors. The details are illustrated in tables and figures for clarity.

### 5.2.1 Calculated Rate of Deposition and Particle Size

The rate of deposition was calculated for different time intervals. One interval spanned Monday to Wednesday, during which Monday's plate was cleaned, ensuring that the dust coverage always started at zero. For the second interval, the rate of deposition was calculated from Wednesday to Friday, using the dust coverage on Wednesday as the initial measurement. Finally, the rate of deposition was calculated using the dust coverage values from Monday and Friday, with Monday having zero dust coverage, assessing the average rate of deposition for the entire work week. The calculated rates of deposition can be viewed in table 5.4. The rate of deposition was calculated using equation 5, all of the codes used for calculations can be viewed in appendix B.2.

Table 5.4: Calculated rate of deposition for varying time intervals

| | **Intervall** | **Date** | **Room 1** | **Room 2** | **Room 3** | **Room 4** | **Unit** |
|---|---|---|---|---|---|---|---|
| Week 1 | Mon-Wed | 19.02-21.02 | 1.16 | 3.34 | 1.52 | 0.96 | 1/h |
| | Wed-Fri | 21.02-23.02 | -0.21 | 0 | 1.31 | 1.07 | 1/h |
| | Mon-Fri | 19.02-23.02 | 0.70 | 2.12 | 1.49 | 1.00 | 1/h |
| Week 2 | Mon-Wed | 04.03-06.03 | - | 1.23 | 0.63 | 0.26 | 1/h |
| | Wed-Fri | 06.03-08.03 | - | -0.31 | 0.69 | 0.17 | 1/h |
| | Mon-Fri | 04.03-08.03 | - | 0.99 | 0.65 | 0.24 | 1/h |
| Week 3 | Mon-Wed | 11.03-13.03 | 1.94 | 4.89 | 3.94 | 1.63 | 1/h |
| | Wed-Fri | 13.03-15.03 | -0.68 | -0.82 | 0.52 | 0.37 | 1/h |
| | Mon-Fri | 11.03-15.03 | 0.53 | 1.51 | 2.03 | 0.92 | 1/h |

The rate of deposition for the four-day intervals, compared to the calculated particle size for the same intervals, can be viewed in Figure 5.3. No obvious trend is discernible from the graph; however, there are indications that smaller particles have a lower deposition rate than the larger ones. The particle sizes was calculated using equation 17. All of the larger particle size (>2.5) calculations came from room 2, which had the lowest proportion of PM2.5 when considering the overall PM10 concentration.

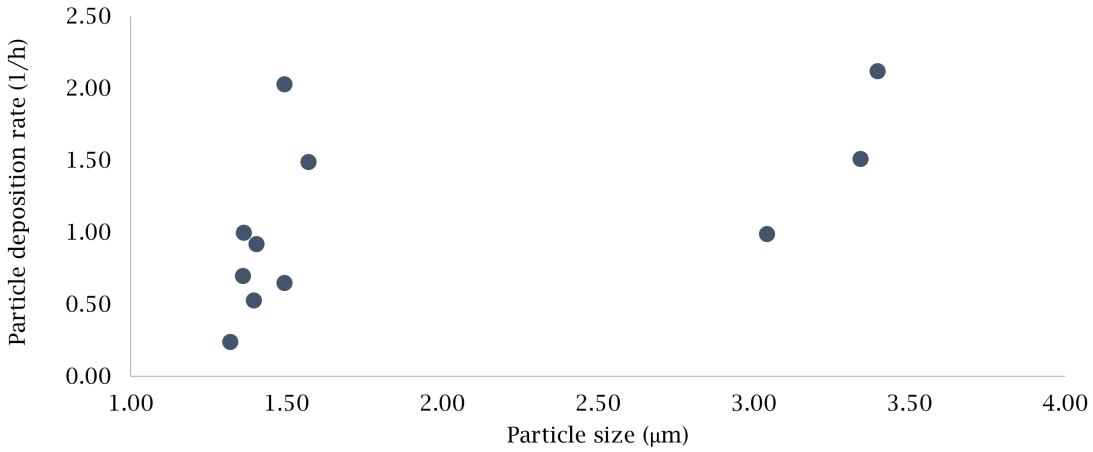


Figure 5.3: Comparison of particle deposition rates and average particle sizes

The calculated rate of deposition for the four-day intervals, compared to the measured dust coverage values, can be seen in Figure 5.4. A notable positive trend is observed: as the dust coverage increases, the particle deposition rate also increases.

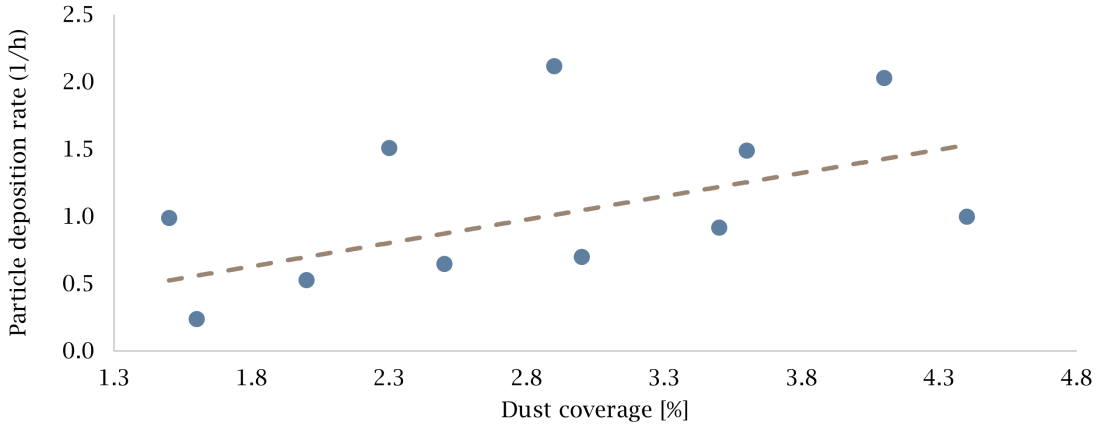


Figure 5.4: Comparison of calculated particle deposition rates and measured dust coverage

### 5.2.2 Calculated Dust Coverage Over Time

Using equation 13, the dust coverage over time can be calculated. The following section present the results for different rooms, divided by week. The figures displaying dust coverage over time combine two graphs: one graph reflects a changing rate of deposition, determined using measurements from Monday and Wednesday, and then from Wednesday to Friday; the other graph, which portrays a constant rate of deposition, is based on measurements from Monday to Friday. The code used for the calculations can be viewed in appendix B.2.

#### Dust coverage, Week 1

For the first week of testing, from 19.02.2024 to 23.02.2024, all the rooms showed a similar trend in PM10 values. However, the measurements for dust coverage percentage varied. Rooms 1 and 2 had lower dust coverage on Friday than on Wednesday, resulting in the graphs with changing rate of deposition having a large variation from to the graphs with a constant rate of deposition. For Rooms 3 and 4, the graph showing a changing rate of deposition is very similar to the graphs with a constant rate of deposition. All of the graphs can be viewed in figures 5.5, 5.6, 5.7 and 5.8.

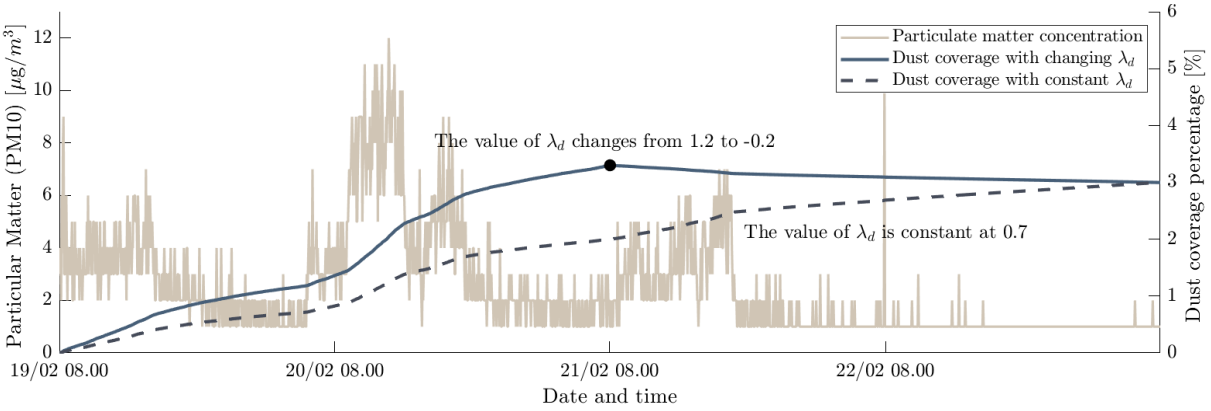


Figure 5.5: PM10 and dust coverage, room 1 week 1

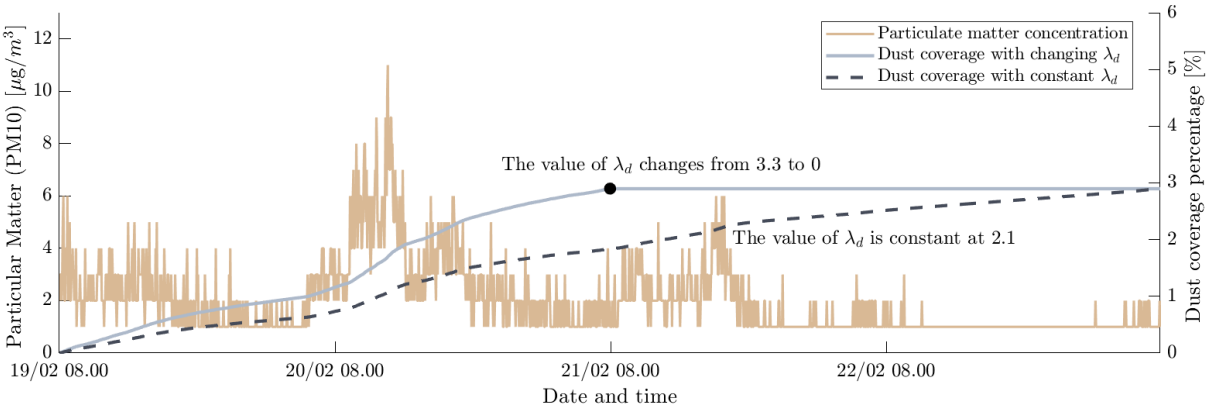


Figure 5.6: PM10 and dust coverage, room 2 week 1

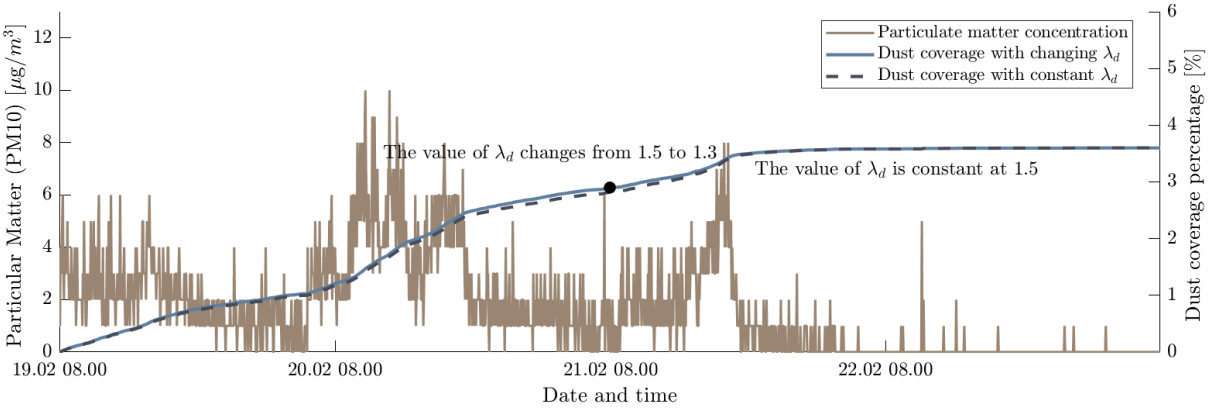


Figure 5.7: PM10 and dust coverage, room 3 week 1

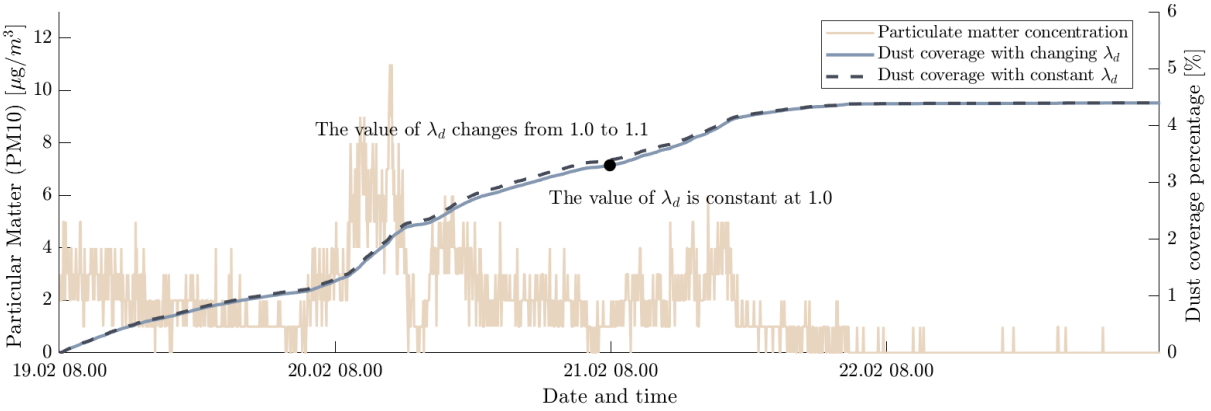


Figure 5.8: PM10 and dust coverage, room 4 week 1

### Dust coverage, Week 2

During the second week of testing, from 04.03.2024 to 08.03.2024, a consistent trend in PM10 values was observed across all rooms, except for Room 1, where a sensor malfunction rendered the data unusable. PM10 levels peaked early in the week and declined until they stabilized at low values by Tuesday morning. Variability in dust coverage percentages was noted among the rooms. Specifically, Room 2 showed a decrease in dust coverage from Wednesday to Friday, resulting in a curve depicting the rate of deposition with significant variation compared to the graph with a constant rate of deposition. Rooms 3 and 4 displayed graphs of changing deposition rates that closely resembled those with constant rates. These graphs can be reviewed in Figures 5.9, 5.10, and 5.11.

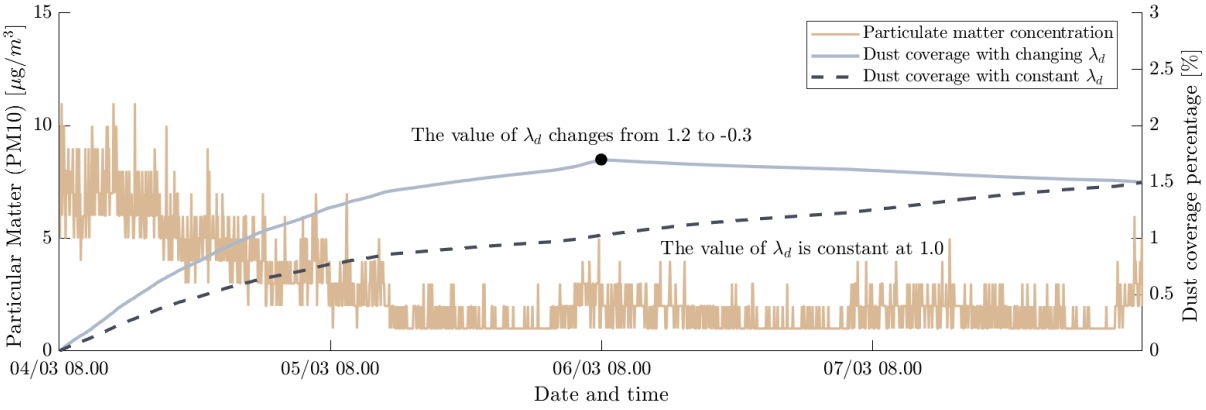


Figure 5.9: PM10 and dust coverage, room 2 week 2

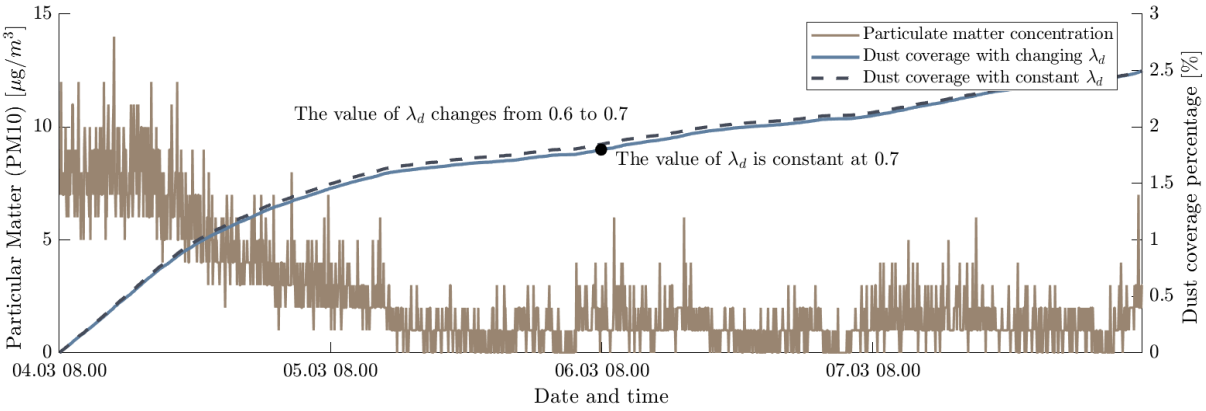


Figure 5.10: PM10 and dust coverage, room 3 week 2

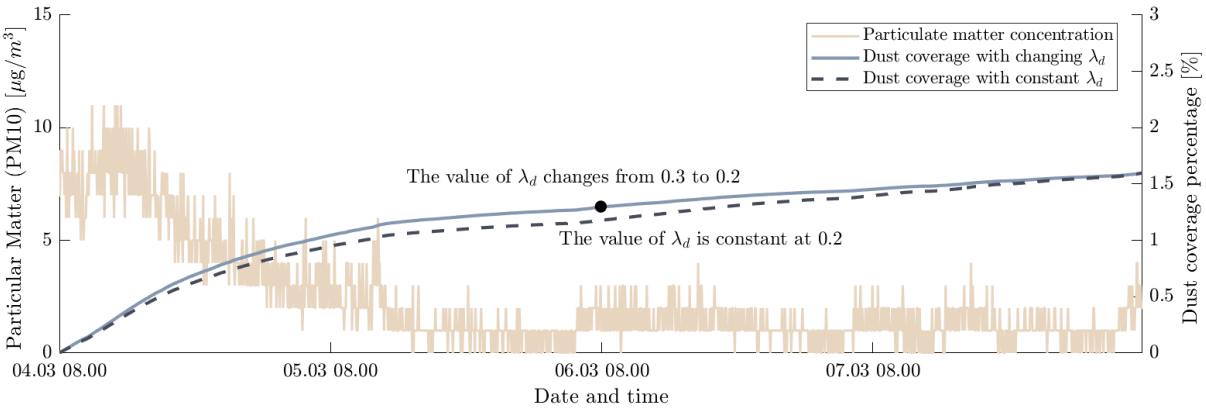


Figure 5.11: PM10 and dust coverage, room 4 week 2

### Dust coverage, Week 3

During the third week of testing, from 11.03.2024 to 15.03.2024, a consistent trend in PM10 values was observed across all rooms. PM10 levels were generally stable at low values, except for a significant increase in all rooms from Wednesday morning until about midday Wednesday. Variability in dust coverage percentages was noted among the rooms. Rooms 3 and 4 had almost double the amount of dust coverage compared to Rooms 1 and 2 on Friday. All rooms exhibited a large variance between the graphs with varying rates of deposition and those with a constant rate of deposition. The graphs can be viewed in Figures 5.12, 5.13, 5.14, and 5.15.

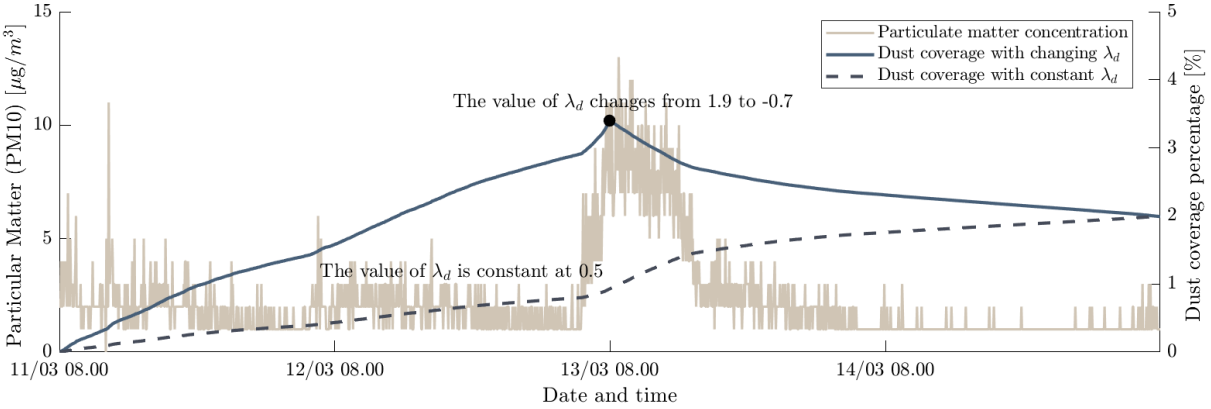


Figure 5.12: PM10 and dust coverage, room 1 week 3

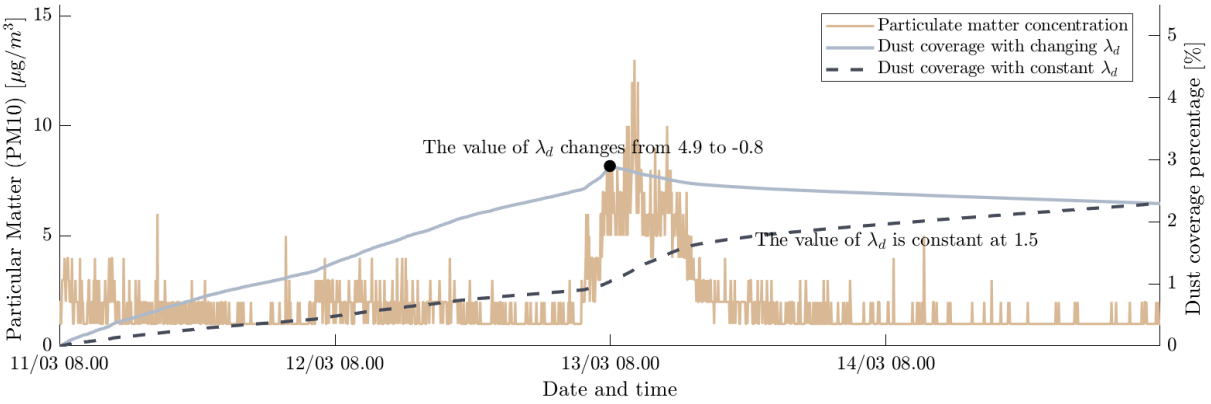


Figure 5.13: PM10 and dust coverage, room 2 week 3

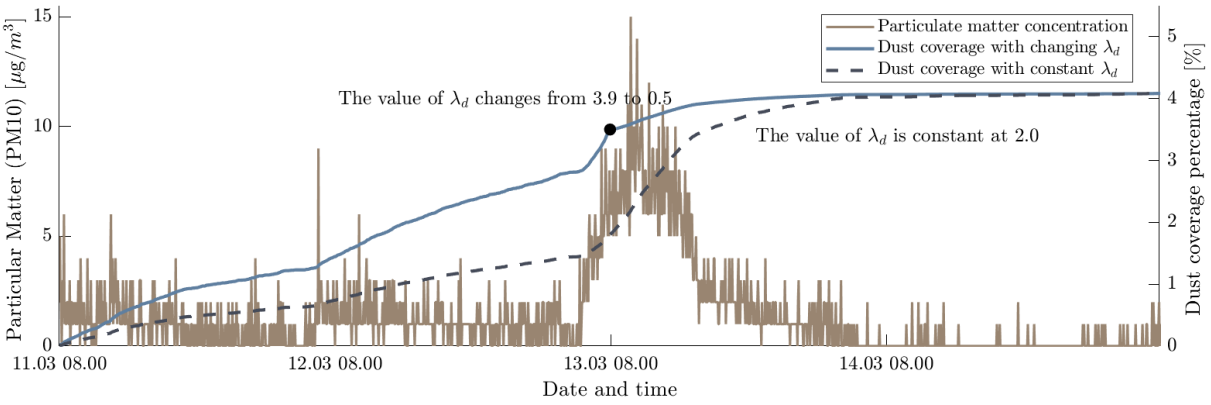


Figure 5.14: PM10 and dust coverage, room 3 week 3

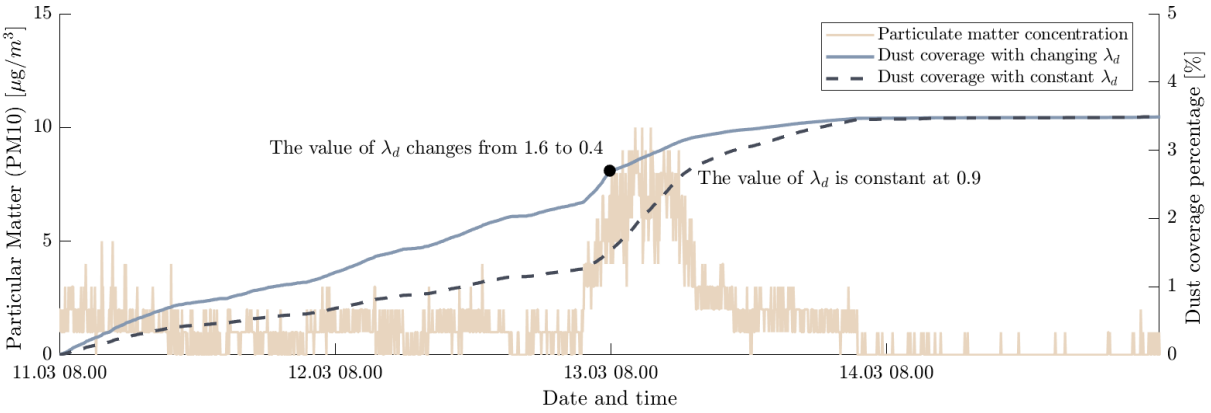


Figure 5.15: PM10 and dust coverage, room 4 week 3

# 6 Discussion

The study aims to quantify and characterize the correlation between airborne particles and particle deposition in Norwegian schools, with the goal of predicting deposition rates from sensor data and ultimately modernizing the cleaning industry. The main research question focuses on understanding how particulate matter levels relate to the deposition of these particles on surfaces. The following chapter examines the results and interprets them in an effort to answer the research question.

## 6.1 Significance of Measured Results

### 6.1.1 Assessing Variability and Reliability in Dust Percentage Measurements

The dust percentage measurements obtained using the BM Dust Detector exhibited a range of results, highlighting the variability inherent in such environmental assessments. To ensure the reliability and consistency of these measurements, three separate samples were taken for each measurement. Significant variation was observed among the three samples collected during each measurement. The details of this variance are documented in Table 5.2. Such large discrepancies between samples can be attributed to several potential factors, each of which could influence the accuracy and consistency of the results. One possible cause of the variance could be the BM Dust Detector itself. Like all scientific instruments, it may have inherent accuracy errors, which can result in differing readings under identical conditions. Additionally, the physical distribution of dust within the environment might not be uniform, leading to variations in sample collection. Uneven dust distribution can occur due to air currents, room layout, and other environmental factors that affect how particulates settle. Human error also presents a significant risk in the process of sample collection and handling. Missteps in protocol, such as inconsistent sample volume or mishandling of the detection equipment, can skew results. Furthermore, the foil used in the measurements, which serves as the substrate for capturing particulates, might vary in its adhesive qualities. Differences in stickiness could lead to inconsistent amounts of dust being collected on the foil, further contributing to the variance observed.

Given these potential sources of error, the average of the three samples was calculated for each measurement session to derive the most reliable indicator of dust levels at each given time and day. A detailed average of the samples for each measurement session is presented in Table 5.1. These measurements showed significant variability when conducted at two-day intervals. Notably, on four separate occasions, the dust levels recorded on Friday were unexpectedly lower than those measured on the preceding Wednesday. This observation stands in stark contrast to the established theoretical framework concerning the deposition of particulate matter.

According to the theoretical basis, the percentage of dust coverage should be directly influenced by two key factors: the indoor concentration of particulate matter and the rate of deposition, see section 3.2.2. A decrease in dust coverage over a two-day period sug-

gests a negative deposition rate. However, this is highly improbable under the conditions observed, where the PM10 values were either stable or exhibited an increase from Wednesday to Friday, rather than a decrease. Typically, the deposition rate should not fall into negative values unless influenced by external forces such as air velocity and turbulence, which were not present in this scenario.

The theory of gravitational settling further supports the expectation that particles should adhere to surfaces over time, leading to an incremental increase in dust coverage, see section 2.3.1. Thus, the observed reduction in dust coverage after two days challenges the conventional understanding of particulate matter behavior under normal gravitational forces. This anomaly shows that there might be unrecognized environmental variables or measurement errors influencing the results.

### 6.1.2 Estimation of Average Particulate Matter Size and Analysis of PM2.5 and PM10 Data

To accurately estimate the average size of particulate matter particles, necessary for calculating the rate of deposition, it was essential to separate the PM2.5 data from the PM10 data. PM2.5 represented more than 80% of the particulate matter in all instances, except for the measurements in Room 2, which displayed a notably lower PM2.5 proportion. The results detailing the PM2.5 share of total particulate matter are presented in Table 5.3. Although Room 2 had a smaller proportion of PM2.5, it still recorded almost the same amount of PM10 as the other rooms, albeit slightly lower. This discrepancy makes it tempting to attribute it to a measuring error or a calibration issue. The data for Room 2 indicated that the PM2.5 measurements were zero for 85% of the time in week 1, 78% in week 2, and 89% in week 3. While the measured data has been further utilized in this study, it is important to note the differences from the other rooms and be wary that it might have been measured incorrectly.

The calculated average size of the particulate matter ranged from a diameter of 1.3 $\mu m$ to 3.4 $\mu m$. Naturally, Room 2 had the largest particle size, all above 3.0 $\mu m$, due to the low PM2.5 share of the total PM10 data.

The sensor in room 1 was down for parts of week 2 and the data could not be used due to being incomplete.

## 6.2 Analysis of Calculated Results

### 6.2.1 Deposition Rates Across Varied Time Intervals and Particle Sizes

The rate of deposition was calculated across different time intervals, each defined to understand the accumulation of dust under varying conditions. Initially, calculations were conducted from Monday to Wednesday, starting with a clean plate on Monday to ensure zero dust coverage at the outset. Subsequently, the rate of deposition from Wednesday to Friday was determined using Wednesday's dust coverage as the baseline measurement. Lastly, the rate of deposition from Monday to Friday was calculated to assess the average rate across the entire workweek, with Monday beginning with zero dust coverage. The results of these calculations are detailed in Table 5.4, utilizing the formula outlined in Equation 5. The deposition rates ranged from -0.82 1/h to 4.89 1/h. As mentioned in Section 6.1.1, the negative values might arise from unrecognized environmental variables or measurement errors. To avoid these negative values and facilitate a better comparison, only the four-day intervals were used when examining the relationship between the deposition rates and the particle sizes.

When comparing the calculated deposition rates with the particle sizes, the graph in Figure 2.1 was employed. The calculated values from this study were added. As shown in Figure 6.1, both the calculated deposition rates and the calculated particle sizes align with what is expected when compared to previous works. The larger particle sizes follow the curve and exhibit a higher deposition rate.

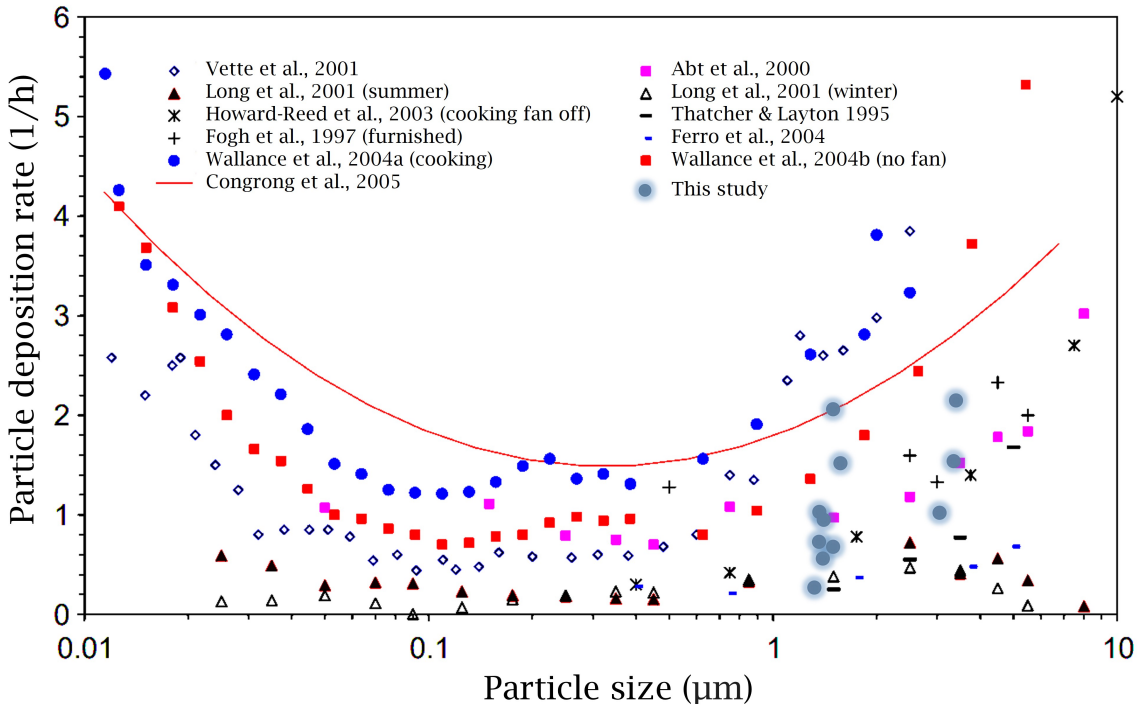


Figure 6.1: Comparison of particle deposition rates reported in literature and this study [13]

The higher deposition rate for larger sizes is natural when considering the equation used to calculate the flow density, Equation 16. This equation utilizes the mass of the particles as well as the cross-sectional area to determine how much weight lands on the collection plate per second. Smaller particles would have lower mass for the same cross-sectional area, as they do not accumulate as much height. This concept is visualized in Figure 6.2, where both scenarios exhibit 100% dust coverage, but the collection plate with the larger particles has significantly more mass collected on top.

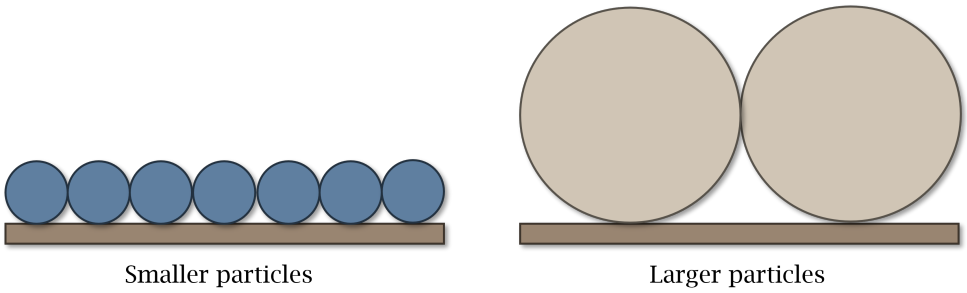


Figure 6.2: Smaller and larger particles covering the same area

Using the IAQ sensors to find the exact particle size at any given time and cross-referencing it with the correct deposition rate according to Figure 6.1 could provide the means to calculate the deposited dust in real time using Equation 4. This approach, however, neglects other parameters such as humidity and air speed.

### 6.2.2 Evaluation of Dust Coverage Influences, Simplifications, and Anomalies

The dust percentage coverage over time is calculated using Equation 13. This equation clearly shows that dust coverage is significantly influenced by the concentration of particulate matter in the air. Higher concentrations in the air result in greater dust deposition, leading to a higher dust percentage coverage. This effect is primarily due to gravitational settling. However, Equation 13 is a highly simplified model that disregards external forces acting on the particles.

Some of these forces are described by Newton's second law of motion, as shown in Equation 1. By neglecting the acceleration of the fluid surrounding the particles, air velocity, turbulence, and relative humidity, the model loses a substantial part of the mechanics influencing deposition, resulting in less reliable outcomes. Despite this, the complexity of particulate matter deposition necessitates certain simplifications. These simplifications, based on previous works and literature, are considered reliable, albeit less precise.

All of the dust coverage graphs that showed a change in deposition rate on Wednesday indicated higher deposition rates from Monday to Wednesday compared to Wednesday to Friday. This discrepancy could have been caused by the collection plate not being completely clean on Monday, resulting in higher dust coverage on Wednesday than was accurate. The cleaning of the plate was tested once to determine the correct method to

use, but due to limited resources, it was not feasible to test that each collection plate was clean before each testing period.

Another reason for the decline in the deposition rate from the first half of the week to the second part of the week is an error in the calculations. Equation 16 does take into account the probability of particles landing on top of each other rather than in the empty spots on the collection plate. However, this equation assumes uniform dust deposition across the collection plate. If the dust deposition has large variations in placement, the equation gives incorrect results.

However, none of these reasons explain why the dust coverage was sometimes lower on Friday compared to Wednesday. For the dust coverage to be lower on Friday than on Wednesday, as it was in Room 1 during weeks one and two, and in Room 2 during weeks two and three, the resuspension rate would have had to be higher than the deposition rate. Considering that the equation used for dust coverage over time, Equation 13, uses a deposition rate that also includes the resuspension rate, it is impossible to determine the exact dynamics behind the reduction in dust coverage.

The abnormally high readings on Wednesdays compared to Fridays cause the graphs describing the dust coverage to be negative during some of the highest PM peaks, as shown in Figure 5.12 and Figure 5.13. This is a highly improbable result, and it can be reasonably assumed that longer testing intervals provide higher accuracy, as the elevated readings in the first few days have less impact when the interval is longer.

The calculated deposition rates for the week-long intervals align with what is found in previous work, as discussed in section 6.2.1, but the calculated size and mass of the particles could be more accurate. If testing were done concerning the elemental composition of the particulate matter in the testing location, the mass of the particles would be more precise, providing a better understanding of the flow rate. The exact size of the particles could also be calculated more accurately if the sensors had data for a larger variance of sizes. If the sensors picked up PM1 and PM5 data in addition to the recorded PM2.5 and PM10, the size calculations would be more accurate, leading to a more exact deposition rate.

# 7 Conclusion

The main research question revolves around quantifying and characterizing the correlation between airborne particles and particle deposition in Norwegian schools in hopes of modernizing the cleaning industry. By finding a link between airborne particulate matter levels and particle deposition rates, cleaning can be done on an as-needed basis instead of at scheduled times. This can increase productivity and reduce costs.

The measurements done with the BM dust detector showed varying results, with dust coverage at times being lower on Friday than on Wednesday, even though there was no cleaning in between. These measurements could be caused by high resuspension rates, but this is unlikely due to no recorded factors that could result in increased resuspension. The elevated measurements on Wednesday were likely due to a measurement error. The longer four-day interval was deemed more accurate, as the readings in the first few days had less impact when the interval was longer. The IAQ sensor showed that a large part of the overall PM had a smaller size, with sensors recording PM2.5 percentages in the high eighties when looking at the overall PM values. Only Room 2 had more PM larger than 2.5 $\mu m$ in diameter rather than smaller. This should be noted when looking at the overall results, as it could be a measurement error from the IAQ sensor.

The particle sizes were used to calculate the particle deposition rate. The calculated rates, when compared to previous works on particle sizes and deposition rates, aligned with what was expected based on the particle sizes. This shows that it is possible to use IAQ sensors to estimate particle deposition rates. If the sensors can obtain even more detailed readings on the particle sizes, it is possible to find the corresponding deposition rate and use this to calculate dust deposition in real time using the recorded PM values in the room.

The calculated deposition rates involve more assumptions than the deposition rates from literature. If the deposition rates are to be calculated instead of cross-referenced with particle sizes, tests should be done regarding the elemental composition of the particulate matter. This is important to determine the exact weight needed to calculate the flow rate for the deposition. However, this process is costly and time-consuming as it must be done manually, which defeats the purpose of using the IAQ sensors to find the dust coverage.

In conclusion, IAQ sensors can provide valuable insights into particle deposition rates, but enhancing the accuracy of particle size calculations and mass measurements is crucial. Improved testing of the elemental composition and obtaining more detailed sensor readings will refine these calculations, enabling real-time dust deposition monitoring. understanding how airborne particulate matter values influence deposition rates could advance and significantly optimize cleaning schedules, increase productivity, and reduce costs in Norwegian schools.

## 7.1 Further Work

Future research should focus on identifying corresponding deposition rates for a wider range of particle sizes. While the current study has provided valuable insights into specific particle size categories, a comprehensive understanding across all possible particle sizes will enhance the accuracy of real-time dust deposition calculations. This can be achieved through extensive experimental measurements and validation against established literature.

To gain a deeper understanding of the correlation between airborne particle levels and particle deposition, additional testing is essential. This includes controlled experiments that account for various environmental factors such as different ventilation systems, air dynamics, and external environmental conditions. By expanding the dataset and refining the experimental setup, it will be possible to obtain more reliable and consistent results, thereby strengthening the observed correlations.

Leveraging machine learning models to predict particulate matter values and their deposition rates represents a promising direction for future research. By training algorithms on the extensive datasets collected from IAQ sensors, it is possible to develop predictive models that can provide real-time insights into particulate matter levels and their expected deposition rates. This predictive capability will facilitate the transition to an as-needed cleaning approach, optimizing resource allocation and further reducing costs.

# Bibliography


[1] Hayder Saadoon Abdulaali et al. “Impact of poor indoor environmental quality (IEQ) to inhabitants’ health, wellbeing and satisfaction”. In: *International Journal of Advanced Science and Technology* 29.3 (2020), pp. 1–14.

[2] Yitayal Addis Alemayehu, Seyoum Leta Asfaw, and Tadesse Alemu Terfie. “Exposure to urban particulate matter and its association with human health risks”. In: *Environmental Science and Pollution Research* 27 (2020), pp. 27491–27506.

[3] Mehzabeen Mannan and Sami G Al-Ghamdi. “Indoor air quality in buildings: a comprehensive review on the factors influencing air pollution in residential and commercial structure”. In: *International Journal of Environmental Research and Public Health* 18.6 (2021), p. 3276.

[4] Iselin Ørbek Eide. “Outdoor Influences on Indoor Particulate Matter Values”. In: (2023).

[5] Ki-Hyun Kim, Ehsanul Kabir, and Shamin Kabir. “A review on the human health impact of airborne particulate matter”. In: *Environment international* 74 (2015), pp. 136–143.

[6] James S Brown et al. “Thoracic and respirable particle definitions for human health risk assessment”. In: *Particle and fibre toxicology* 10 (2013), pp. 1–12.

[7] Richard W Atkinson et al. “Urban ambient particle metrics and health: a time-series analysis”. In: *Epidemiology* (2010), pp. 501–511.

[8] Jakob Löndahl et al. “A set-up for field studies of respiratory tract deposition of fine and ultrafine particles in humans”. In: *Journal of Aerosol Science* 37.9 (2006), pp. 1152–1163.

[9] Direktoratet for byggkvalitet. *Byggteknisk forskrift (TEK17)*. https://www.dibk.no/regelverk/byggteknisk-forskrift-tek17. Accessed: 2023-04-03. 2017.

[10] Lovdata. *Forskrift om begrensning av forurensning*. https://lovdata.no/dokument/SF/forskrift/2004-06-01-931. Accessed: 2024-04-05. 2004.

[11] Folkehelseinstituttet (FHI). *Nye luftkvalitetskriterier for svevestøv og nitrogendioksid*. https://www.fhi.no/meldinger/nye-luftkvalitetskriterier-for-svevestov-og-nitrogendioksid/. Accessed: 2024-04-05. 2023.

[12] Kompetansehuset Neo. *Hva er NS-INSTA 800?* Accessed: 2024-05-23. 2023. URL: https://blogg.kompetansehusetneo.no/hva-er-ns-insta-800.

[13] Congrong He, Lidia Morawska, and Dale Gilbert. “Particle deposition rates in residential houses”. In: *Atmospheric Environment* 39.21 (2005), pp. 3891–3899.

[14] Tracy L Thatcher et al. “Effects of room furnishings and air speed on particle deposition rates indoors”. In: *Atmospheric environment* 36.11 (2002), pp. 1811–1819.

[15] WJ Trompetter et al. “The effect of ventilation on air particulate matter in school classrooms”. In: *Journal of Building Engineering* 18 (2018), pp. 164–171.

[16] J-M Lim et al. “The analysis of PM2. 5 and associated elements and their indoor/outdoor pollution status in an urban area”. In: *Indoor Air* 21.2 (2011), pp. 145–155.

[17] Spyros Karakitsios et al. “Integrated exposure for risk assessment in indoor environments based on a review of concentration data on airborne chemical pollutants in domestic environments in Europe”. In: *Indoor and Built Environment* 24.8 (2015), pp. 1110–1146.

[18] Melvin W First. “HEPA filters”. In: *Journal of the American Biological Safety Association* 3.1 (1998), pp. 33–42.

[19] Yunlong Han, Yongmei Hu, and Fuping Qian. “Effects of air temperature and humidity on particle deposition”. In: *Chemical Engineering Research and Design* 89.10 (2011), pp. 2063–2069.

[20] Morton Corn and Felix Stein. “Re-entrainment of particles from a plane surface”. In: *American Industrial Hygiene Association Journal* 26.4 (1965), pp. 325–336.

[21] Yakov I Rabinovich et al. “Capillary forces between surfaces with nanoscale roughness”. In: *Advances in colloid and interface science* 96.1-3 (2002), pp. 213–230.

[22] Joshua A Hubbard et al. “Experimental study of impulse resuspension with laser Doppler vibrometry”. In: *Aerosol Science and Technology* 46.12 (2012), pp. 1303–1312.

[23] Evdokia Stratigou et al. “Investigation of PM10, PM2. 5, PM1 in an unoccupied airflow-controlled room: How reliable to neglect resuspension and assume unreactive particles?” In: *Building and Environment* 186 (2020), p. 107357.

[24] G Ziskind, M Fichman, and Ch Gutfinger. “Resuspension of particulates from surfaces to turbulent flows—review and analysis”. In: *Journal of aerosol science* 26.4 (1995), pp. 613–644.

[25] Bin Hu et al. “Literature review and parametric study: Indoor particle resuspension by human activity”. In: *Proceedings of Indoor Air* 2005 (2005).

[26] F Mazzei et al. “Characterization of particulate matter sources in an urban environment”. In: *Science of the total environment* 401.1-3 (2008), pp. 81–89.

[27] Arideep Mukherjee and Madhoolika Agrawal. “World air particulate matter: sources, distribution and health effects”. In: *Environmental chemistry letters* 15 (2017), pp. 283–309.

[28] Viney P Aneja, William H Schlesinger, and Jan Willem Erisman. “Farming pollution”. In: *Nature Geoscience* 1.7 (2008), pp. 409–411.

[29] Sujit Das, Debanjana Pal, and Abhijit Sarkar. “Particulate matter pollution and global agricultural productivity”. In: *Sustainable Agriculture Reviews 50: Emerging Contaminants in Agriculture* (2021), pp. 79–107.

[30] Ling Zhang et al. “Indoor particulate matter in urban households: sources, pathways, characteristics, health effects, and exposure mitigation”. In: *International Journal of Environmental Research and Public Health* 18.21 (2021), p. 11055.

[31] David A Sterling et al. “Evaluation of four sampling methods for determining exposure of children to lead-contaminated household dust”. In: *Environmental research* 81.2 (1999), pp. 130–141.

[32] Diana Meza-Figueroa, Margarita De la O-Villanueva, and Maria Luisa De la Parra. “Heavy metal distribution in dust from elementary schools in Hermosillo, Sonora, México”. In: *Atmospheric Environment* 41.2 (2007), pp. 276–288.

[33] Suzanne Beauchemin et al. “Quantification and characterization of metals in ultrafine road dust particles”. In: *Atmosphere* 12.12 (2021), p. 1564.

[34] Pawel Markowicz and Lennart Larsson. “Improving the indoor air quality by using a surface emissions trap”. In: *Atmospheric Environment* 106 (2015), pp. 376–381.

[35] Norges Astma- og Allergiforbund. *Muggsopp og Støv Analyse med MycoTape DNA*. Accessed: 2024-06-06. 2024. URL: https://www.naaf.no/stott-oss/bli-medlem/medlemsfordeler/muggsopp-og-stov-analyse-med-mycotape-dna.

[36] Thomas Schneider et al. “A simple method for the measurement of dust on surfaces and the effectiveness of cleaning”. In: *Environment International* 15.1-6 (1989), pp. 563–566.

[37] Zuocheng Wang et al. “Comparison of real-time instruments and gravimetric method when measuring particulate matter in a residential building”. In: *Journal of the Air & Waste Management Association* 66.11 (2016), pp. 1109–1120.

[38] Benjamin Chu. *Laser light scattering: basic principles and practice*. Courier Corporation, 2007.

[39] Imre Balásházy, Ted B Martonen, and Werner Hofmann. “Inertial impaction and gravitational deposition of aerosols in curved tubes and airway bifurcations”. In: *Aerosol science and technology* 13.3 (1990), pp. 308–321.

[40] Suresh Aggarwal, Y Xiao, and J Uthuppan. “Effect of Stokes number on particle dispersion”. In: *Atomization and Sprays* 4.2 (1994).

[41] Philip Lengweiler. “Modelling Deposition and Resuspension of Particles on and from Surfaces”. PhD thesis. ETH Zurich, 2000.

[42] Aikaterini Sfakianaki et al. “Study on particles’ mass balance as a function of the ventilation rate in a test cell”. In: (2009).

[43] Tracy L Thatcher and David W Layton. “Deposition, resuspension, and penetration of particles within a residence”. In: *Atmospheric environment* 29.13 (1995), pp. 1487–1497.

[44] Sameer Patel et al. “Indoor particulate matter during HOMEChem: Concentrations, size distributions, and exposures”. In: *Environmental science & technology* 54.12 (2020), pp. 7107–7116.

[45] Kontur AS. *Lundstein Skole*. Accessed: 2024-05-28. 2024. URL: https://www.kontur.as/lundstein-skole.

# Appendix

## A Dust Coverage Measurements

All dust coverage measurements

| | Date | Measurement | Room 1 | Room 2 | Room 3 | Room 4 |
|---|---|---|---|---|---|---|
| **Week 1** | **Date: 21.02** | M1 | 4.7 | 3.8 | 3.1 | 3.1 |
| | | M2 | 2.6 | 3.1 | 1.4 | 6.2 |
| | | M3 | 2.5 | 1.8 | 4.2 | 0.6 |
| | **Average** | | **3.3** | **2.9** | **2.9** | **3.3** |
| | **Variance** | | 1.5 | 1.0 | 2.0 | 7.9 |
| | **Date: 23.02** | M1 | 5.3 | 3.7 | 5.9 | 5.2 |
| | | M2 | 1.8 | 2.3 | 3.3 | 3.3 |
| | | M3 | 1.9 | 2.7 | 1.5 | 4.6 |
| | **Average** | | **3.0** | **2.9** | **3.6** | **4.4** |
| | **Variance** | | 4.0 | 0.5 | 4.9 | 0.9 |
| **Week 2** | **Date: 06.03** | M1 | 2.8 | 2.3 | 2.3 | 1.5 |
| | | M2 | 0.7 | 2.0 | 1.3 | 1.2 |
| | | M3 | 1.1 | 0.8 | 1.7 | 1.3 |
| | **Average** | | **1.5** | **1.7** | **1.8** | **1.3** |
| | **Variance** | | 1.2 | 0.6 | 0.3 | 0.0 |
| | **Date: 08.03** | M1 | 4.8 | 1.2 | 2.1 | 1.1 |
| | | M2 | 2.3 | 1.9 | 2.5 | 1.7 |
| | | M3 | 2.9 | 1.3 | 2.9 | 2.0 |
| | **Average** | | **3.3** | **1.5** | **2.5** | **1.6** |
| | **Variance** | | 1.7 | 0.1 | 0.2 | 0.2 |
| **Week 3** | **Date: 13.03** | M1 | 5.5 | 2.5 | 4.9 | 2.9 |
| | | M2 | 2.0 | 3.5 | 2.7 | 2.5 |
| | | M3 | 2.7 | 2.6 | 3.0 | 2.6 |
| | **Average** | | **3.4** | **2.9** | **3.5** | **2.7** |
| | **Variance** | | 3.4 | 0.3 | 1.4 | 0.0 |
| | **Date: 15.03** | M1 | 1.3 | 2.8 | 4.4 | 2.9 |
| | | M2 | 2.2 | 1.0 | 4.4 | 4.5 |
| | | M3 | 2.5 | 3.0 | 3.6 | 3.1 |
| | **Average** | | **2.0** | **2.3** | **4.1** | **3.5** |
| | **Variance** | | 0.4 | 1.2 | 0.2 | 0.8 |

# B Matlab Codes

The Matlab codes were almost the same for all the calculated results but used different input files depending on the location and date examined. The codes in the appendix are just one of these files.

## B.1 Particulate Matter Size Code

```
filePath = 'filepath';
data=readtable(filePath);
data.Var1 = datetime(data.Var1, 'InputFormat', 'dd/MM/yyyy HH:mm:ss');
%% Particle size
pm_25 = xlsread('filepath');
pm_25_week = pm_25(3292:5211,1);      % PM2.5 Âţg/mÂş
tot_25_week = sum(pm_25_week);
pm_10_week =data{3315:5234, 2}';      % PM10 Âţg/mÂş
tot_10_week = sum(pm_10_week);
part_25_week =tot_25_week/tot_10_week;
avg_d_25=(2.5*10^(-6))/2 %dia
avg_d_10=((10-2.5)*10^(-6))/2
d_week=part_25_week*avg_d_25+(1-part_25_week)*avg_d_10; % average diameter
r_week=d_week/2; % average radius

r1=r_week;

dens = 1000; %kg/m^3
mp= Vp*dens; % kg/n
```

## B.2 Deposition Rate Code

```
filePath = 'filepath';
data=readtable(filePath);
data.Var1 = datetime(data.Var1, 'InputFormat', 'dd/MM/yyyy HH:mm:ss');

%%
S= 1; %35.8 ;%surface area
Sa= 0.21*0.297; %surface collecion plate
V= 1; %89.5 ;%volume

Ap= pi*(r1^2);
Vp=4/3*pi*r1^3;
```

```
12
13 S0=73.6; %surface area room
14 V0=184; % volume room
15
16 %% MONDAY - WEDNESDAY
17 Dc_ons= 2.9/100; % measured dust coverage
18 filteredData_ons = data(3315:4274, :);
19 Ci_ons =data{3315:4274, 2}'; %concentration
20 tid_ons= 960; % time, same size as Ci vector
21 t_ons = 0:1:959; % time vector
22
23 Ci_avg_ons=mean(Ci_ons)*10^(-9); %average concentration in kg/m
       ^3
24 J_ons=(Dc_ons)/(Ap*(tid_ons))*mp; %kg/(m^2*s)
25 Vd_avg_ons=J_ons/Ci_avg_ons; %Speed of deposition m/s
26 a_ons=(S*Vd_avg_ons)/V; %rate of deposition
27
28 r=0;
29 Phi0_ons = 0; % Initial condition for Phi
30
31 integralCi_ons = zeros(size(t_ons));
32
33 % Numerically integrate Ci(t) * exp(r*t) over t
34 for i = 1:length(t_ons)
35     integralCi_ons(i) = trapz(t_ons(1:i), Ci_ons(1:i) .* exp(r *
           t_ons(1:i)));
36 end
37
38 integralCi_ons=integralCi_ons*10^(-9);
39
40 % Calculate Phi(t) using the derived formula
41 Phi_ons = (Phi0_ons + a_ons * integralCi_ons) .* exp(-r*t_ons);
42
43 pros_ons=(Phi_ons*Ap)/(mp)*100;
44
45 %% wEDNESDAY - FRIDAY
46 Dc_fre= 0.7/100; % measured dust coverage difference from
       wednesday
47 filteredData_fre = data(4275:5234, :);
48 Ci_fre =data{4275:5234, 2}'; %concentration
49 tid_fre= 960; % time, same size as Ci vector
50 t_fre = 0:1:959; % time vector
51
52 Ci_avg_fre=mean(Ci_fre)*10^(-9); %average concentration in kg/m
       ^3
```

```
J_fre=(Dc_fre)/(Ap*(tid_fre))*mp; %kg/(m^2*s)
Vd_avg_fre=J_fre/Ci_avg_fre; %Speed of deposition m/s
a_fre=(S*Vd_avg_fre)/V; %rate of deposition

r=0;
Phi0_fre = Phi_ons(end); % Initial condition for Phi

integralCi_fre = zeros(size(t_fre));

% Numerically integrate Ci(t) * exp(r*t) over t
for i = 1:length(t_fre)

    integralCi_fre(i) = trapz(t_fre(1:i), Ci_fre(1:i) .* exp(r *
        t_fre(1:i)), 2); % integralCi_fre(i) = trapz(t_fre(1:i),
        Ci_fre(1:i) .* exp(r * t_fre(1:i)));
end

integralCi_fre=integralCi_fre*10^(-9);

% Calculate Phi(t) using the derived formula
Phi_fre = (Phi0_fre + a_fre * integralCi_fre) .* exp(-r*t_fre);

pros_fre=(Phi_fre*Ap)/(mp)*100;
%% MONDAY - FRIDAY

filteredData_week = data(3315:5234, :);
Ci_week =data{3315:5234, 2}'; %concentration
%RH_week=data{3340:5258, 5}'; %concentration
%CO2_week=data{3340:5258, 3}';
tid_week= 1920; % time, same size as Ci vector
t_week = 0:1:1919; % time vector
Dc_week= 0.036; %measured dust coverage Friday


Ci_avg_week=mean(Ci_week)*10^(-9); %average concentration in kg/
    m^3

J_week=(Dc_week*1)/(Ap*tid_week)*mp;
Vd_avg_week=J_week/Ci_avg_week; %Speed of deposition
a_week=S/V*Vd_avg_week; %rate of deposition

r = 0;
Phi0_week = 0; % Initial condition for Phi

integralCi_week = zeros(size(t_week));
```

```
95
96  % Numerically integrate Ci(t) * exp(r*t) over t
97  for i = 1:length(t_week)
98      integralCi_week(i) = trapz(t_week(1:i), Ci_week(1:i) .* exp(
        r * t_week(1:i)));
99  end
100
101 integralCi_week=integralCi_week*10^(-9);
102
103 % Calculate Phi(t) using the derived formula
104 Phi_week = (Phi0_week + a_week * integralCi_week) .* exp(-r*
    t_week);
105
106 pros_week=(Phi_week*Ap)/(mp)*100;
107
108
109
110 %% theoretical and measured man-ons
111 t0=48;
112
113 J_f_ons=((1+Dc_ons/2)*Dc_ons)/(Ap*(t0))*mp; %kg/(m^2*s)
114 Vd_avg_f_ons=J_f_ons/Ci_avg_ons; %Speed of deposition m/s
115 a_f_ons=(S0*Vd_avg_f_ons)/V0/100; %rate of deposition
116
117 J_f_ons1=(Dc_ons)/(Ap*(48))*mp; %kg/(m^2*s)
118 Vd_avg_f_ons1=J_f_ons1/Ci_avg_ons; %Speed of deposition m/s
119 a_f_ons1=(S0*Vd_avg_f_ons1)/V0; %rate of deposition
120
121 a_t_ons=6.86; %m/s
122 Vd_t_ons=a_t_ons*V0/S0;
123 J_t_ons=Vd_t_ons*Ci_avg_ons;
124 Dc_t_ons=J_t_ons*Ap*(t0)/mp*100;
125
126 J_ons_t=(Dc_t_ons)/(Ap*(tid_ons))*mp; %kg/(m^2*s)
127 Vd_avg_ons_t=J_ons_t/Ci_avg_ons; %Speed of deposition m/s
128 a_ons_t=(S*Vd_avg_ons_t)/V; %rate of deposition
129
130 Phi_ons_t = (0 + a_ons_t * integralCi_ons) .* exp(-r*a_ons_t);
131
132 pros_ons_t=(Phi_ons_t*Ap)/(mp)*100;
133
134 %% theoretical and measured on-fre
135 Phi0_fre_t = Phi_ons_t(end);
136 t0=48;
137
```

```
J_f_fre=((1+Dc_fre/2)*Dc_fre)/(Ap*(t0))*mp; %kg/(m^2*s)
Vd_avg_f_fre=J_f_fre/Ci_avg_fre; %Speed of deposition m/s
a_f_fre=(S0*Vd_avg_f_fre)/V0/100; %rate of deposition


a_t_fre=6.86/3600; %m/s
Vd_t_fre=a_t_fre*V0/S0;
J_t_fre=Vd_t_fre*Ci_avg_fre;
Dc_t_fre=J_t_fre*Ap*(t0)/mp*100;

J_fre_t=(Dc_t_fre)/(Ap*(tid_fre))*mp; %kg/(m^2*s)
Vd_avg_fre_t=J_fre_t/Ci_avg_fre; %Speed of deposition m/s
a_fre_t=(S*Vd_avg_fre_t)/V; %rate of deposition


Phi_fre_t = (Phi0_fre_t + a_fre_t * integralCi_fre) .* exp(-r*
    a_fre_t);

pros_fre_t=(Phi_fre_t*Ap)/(mp)*100;

%% theoretical and measured week
Phi0_week_t = 0;
Dc_week_t=Dc_week;
t0=96;

J_f_week=((1+Dc_week_t/2)*Dc_week_t)/(Ap*(t0))*mp; %kg/(m^2*s)
Vd_avg_f_week=J_f_week/Ci_avg_week; %Speed of deposition m/s
a_f_week=(S0*Vd_avg_f_week)/V0/100; %rate of deposition
```

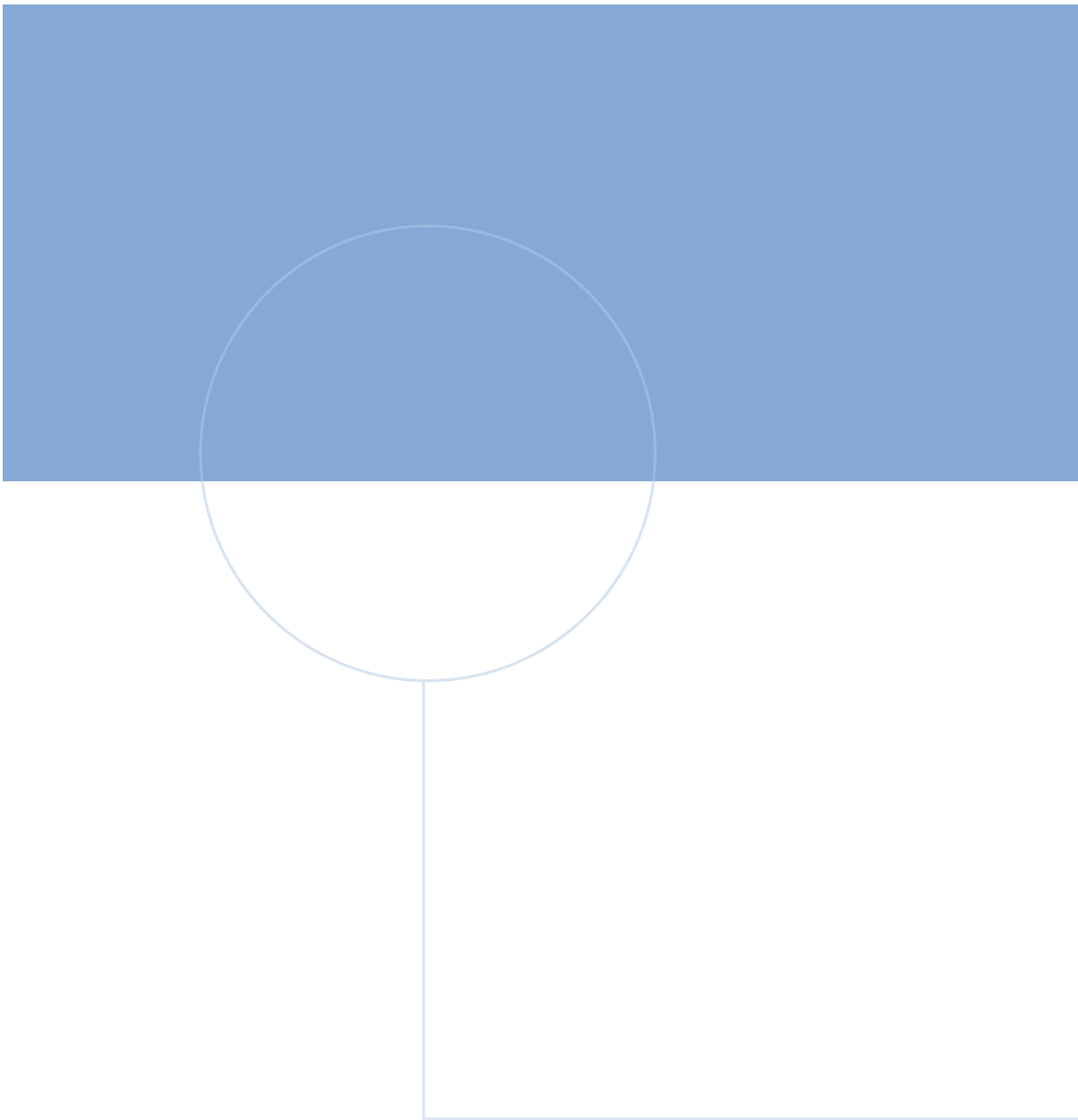

NTNU

Norwegian University of
Science and Technology